



A Review of Bone Regeneration Mechanisms and Bone Scaffold Fabrication Techniques (Conventional and Non-Conventional)

Ali Imran Ansari¹ · Nazir Ahmad Sheikh¹

Received: 1 September 2021 / Accepted: 12 September 2022 / Published online: 28 September 2022
© The Institution of Engineers (India) 2022

Abstract Bone is presently one of the most transplanted tissues with about 15 million fracture cases annually. Bone repair options include Human bone materials (allografts), animal bone materials (xenografts). However, issues such as pain, infection, and immunological rejection have aided in the development of artificial scaffolds such as bone. Autographs and allografts have been utilized for some time in clinical practice; however, they do have problems. The consequences of bone surgical operations may be suboptimal due to intrinsic limitations in the precision and replicability of traditional scaffolding techniques. Despite advancements in bone tissue technology, which provide an impressive instrument for bone replacement, this remains a challenge. Rapid prototyping technologies are an alternative and widely utilized in bone tissue procedures, boosting mechanical strength, porosity geometry, and bioactive components of tissue regeneration while removing some of the drawbacks of previous technologies. This paper discusses the fundamental principles and characteristics of various bone tissue repair mechanisms, as well as traditional and non-traditional fabrication technologies such as freeze-drying procedures, gases foaming, stereolithography, selective laser sintering, and fused deposition modeling, as well as challenges encountered during RPs methods. Tissue scaffolds made with rapid prototyping technologies could be a viable treatment option for bone abnormalities in the future.

Keywords 3D-printing · Bone tissue and repair · Osteocyte function · Melt–dissolution deposition technique · Robocasting

Introduction

With about 15 million fracture cases per year, bone is currently one of the most transplanted tissues. Human bone materials (allografts) and animal bone materials (xenografts) are two options for bone repair. However, issues such as pain, infection, and immunological rejection have aided in the development of artificial scaffolds that are similar to bone [1]. The 3D matrix that allows and stimulates osteoinducible cells to connect and proliferate on their surfaces is known as a bone scaffold. One important aspect of the scaffold design process to consider is that they should promote vascularization and the production of extracellular matrices. They must transfer the load to the adjacent tissues in the most "natural" way possible [2]. The scaffold must be "biocompatible," which means it must pass a cytotoxicity test, keep cells alive, and make them "feel" like a living being. The second requirement, however, is less important but must be considered: the scaffolds must provide good cell attachment. Finally, this structure should be placed in a bioreactor, which means it must be strong enough to withstand mechanical stresses. Fig. 1 describes the various characteristics of a suitable scaffold for use in bone tissue engineering [3]. Knowledge of bone biology and physiology is required to create a proper representation of bone for the purpose of designing biomimetic scaffolds. Bone is a complex open cell composite made up of proteins, growth factors, calcium mineral hydroxyapatite, and a complex vascular system [4]. Bone is made up of three types of cells: mononucleate osteoblasts that form bone, osteoblast-derived osteocytes that are

✉ Ali Imran Ansari
aliimran_06phd19@nitsri.net

¹ Mechanical Engineering Department, National Institute of Technology Srinagar, Srinagar, India

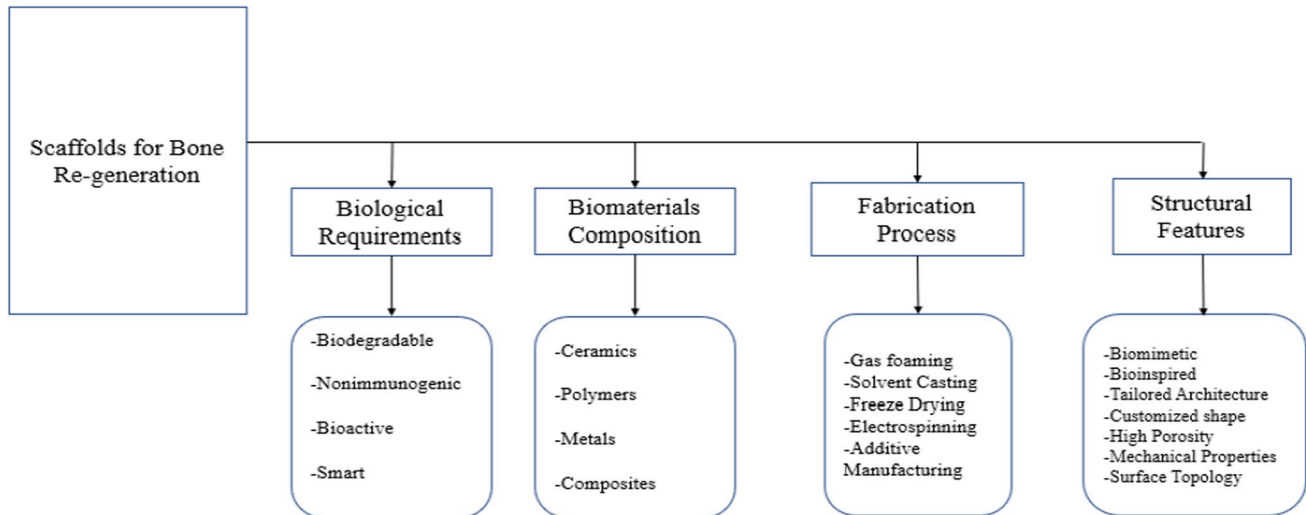


Fig. 1 Characteristics of an appropriate scaffold for bone tissue engineering applications [3]

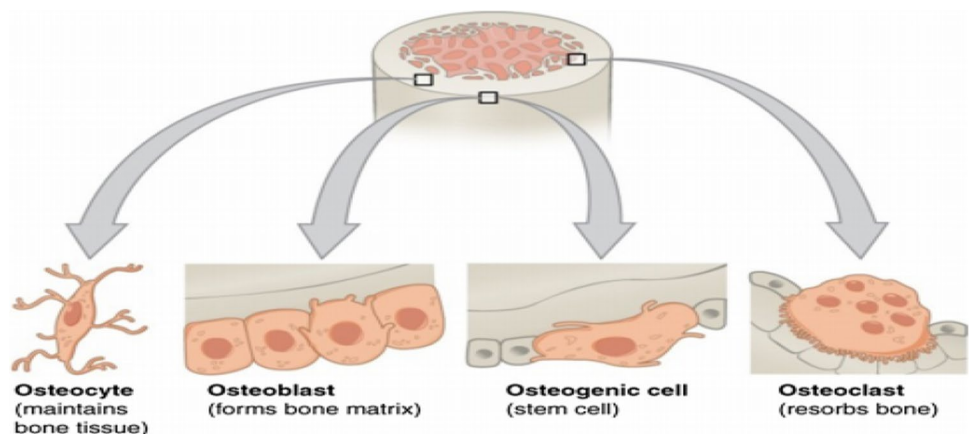
likely mechanical strain sensors, and osteolytic cells. The osteolysis process is used to break down the bone matrix. Both cells are of the mesenchymal type. The third type of cell is osteoclasts, which are multi-nuclear cells that belong to the macrophage family and form blood monocytes. As a result, hematopoietic stem cells produce this cell type. It is the cause of bone ECM degeneration, and the ability of scaffolds to interact with living tissues is one of their most important properties. It is known as scaffold bioactivity. The goal of creating and using bioactive scaffolds is to promote cell migration and differentiation, tissue neof ormation, and host integration while avoiding scarring [5].

Brief Overview on Bone Tissue and Repair

Bone is made up of living bone cells that are organized in a biomineral matrix rather than being a solid mass. The formation of bone is caused by the reinforcement of this

medium in the region of entangled cells. Collagen fibers and inorganic bone minerals in the form of tiny crystals make up the majority of bone. The biomineral medium of bone is composed of roughly 30% organic and 70% inorganic components. More than 90% of this organic segment is collagen, with the remaining 10% consisting primarily of non-collagenous proteins, lipids, proteoglycan molecules, osteopontin (OPN), and other bone matrix proteins. Bone matrix proteins' mechanical strength and tissue adhesion properties are crucial. Hexagonal hydroxyapatite (HA) crystals are the mineral phase of bone. Bone serves a variety of functions in the body, including mechanical (protection, shape, movement, and mobility), synthetic (blood cell generation), and metabolic (energy production) functions (mineral storage, calcium and phosphate management, fat storage). The four most important bone regeneration and structure cells are depicted in Fig. 2: osteogenic, osteoblasts, osteocytes, and osteoclasts (collectively known as the basic multicellular unit) (BMU) [6].

Fig. 2 Four cell types are found in bone tissue: the osteogenic, osteocyte and osteoblast cells [6]



Bone Structure and Bone Cells Regeneration Process

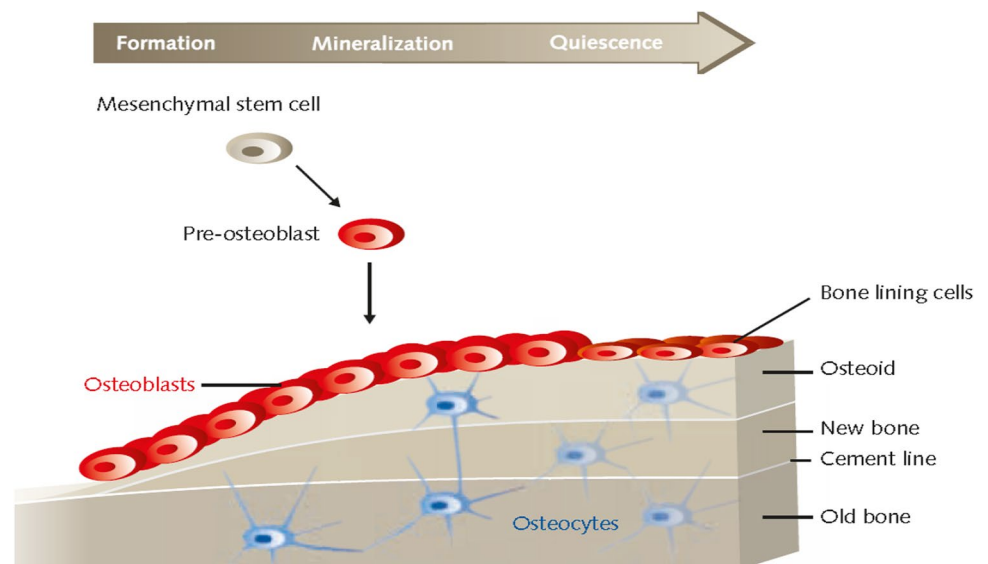
Osteoblasts are cuboidal cells found on the surface of the bone that account for 4–6% of total resident cells. Mesenchyme stem cells (MSC) give rise to osteoblasts. Pre-transition osteoblasts are distinguished by an increase in osterix (osx) expression and secretion of bone matrix proteins (OCN), I/II bone-sip-protein (BSP), and collagen type I. Furthermore, morphological changes are occurring in the osteoblasts, which are transforming into giant cuboidal cells. Osteoblasts synthesize bone matrix in two stages: organic matrix deposition and subsequent mineralization. In the early phase, osteoblasts secrete collagen proteins, which help to create the organic matrix. Following that, bone matrix mineralization occurs in two phases: vesicular and fibrillar (Fig. 3) [7]. When proteoglycan degrading enzymes secrete osteoblasts, calcium ions are released, and the calcium channels in the membrane of the matrix vesicle are covered by proteoglycans. These are the proteins known as annexes [8]. Phosphate-containing compounds, on the other hand, have been extracted by ALP and released by osteoblasts into matrix vesicles. Inside the vesicles, phosphate and calcium ions nucleate to create hydroxyapatite crystals as shown in Fig. 4 [9]. Mature osteoblasts appear to be a single layer of cuboidal cells with a dense coating of rough endoplasm and Golgi complexes. Several of these osteoblastic processes progress to osteocyte processes, where they display cytoplasm in the bone matrix [10]. The mature osteoblast may be apoptosis, osteocytes, or bone lining cells at this stage. The flat, calm osteoblasts that cover the bone surfaces where there is no bone resorption or creation are known as bone lining cells. Their cytoplasm covers the entire surface of the bone and contains a few cytoplasmic organelles like

raw endoplasmic reticulum profiles and Golgi appliances. These cells have a thin and flat nuclear profile [11].

Osteocytes, which account for 90–95% of total bone cells, are the most numerous and long-lived cells, with a life span of up to 25 years. Osteocytes can respond to mechanical strain and send signals of bone formation or resorption to the bone surface, as well as govern both local and systemic mineral homeostasis. Osteocytes are formed through the differentiation of osteoblasts from the MSC lineage [12]. Osteoid-osteocyte, re-osteocyte, young osteocyte, and mature osteocyte are the four stages of this process. After the bone development cycle is completed, a subpopulation of osteoblasts is integrated into the bone matrix. The osteoblast then undergoes significant morphological and ultrastructural changes, such as roundness reduction [13]. The number of organelles such as the rough endoplasmic reticulum and the Golgi apparatus, as well as the nucleus-to-protein synthesis and secretion penetration ratios, decreases [14]. The cytoplasmic process begins before the osteoblasts are encased in the bone matrix, during the osteoblast/osteocyte transition.

An osteocyte's surface area is 400 times that of the Haversian and Volkmann systems, and over 100 times that of trabecular bone. Osteocytes perform mechanosensitive functions because of their optimal placement within the bone matrix. As a result, the osteocytes' shape and spatial arrangement are compatible with their sensor and signal conveyance functions, enabling the piezoelectric effect, in which mechanical stimuli are translated into biochemical signals [15]. In osteocytes, the mechanisms and components that translate mechanical impulses into biochemical signals are unknown. However, two processes have been proposed. One of these is a protein complex composed of cilia and the related proteins PolyCystins 1 and 2, which has been linked to osteoblast/osteocyte-mediated bone formation

Fig. 3 The development and mineralization of osteoblast bone [7]



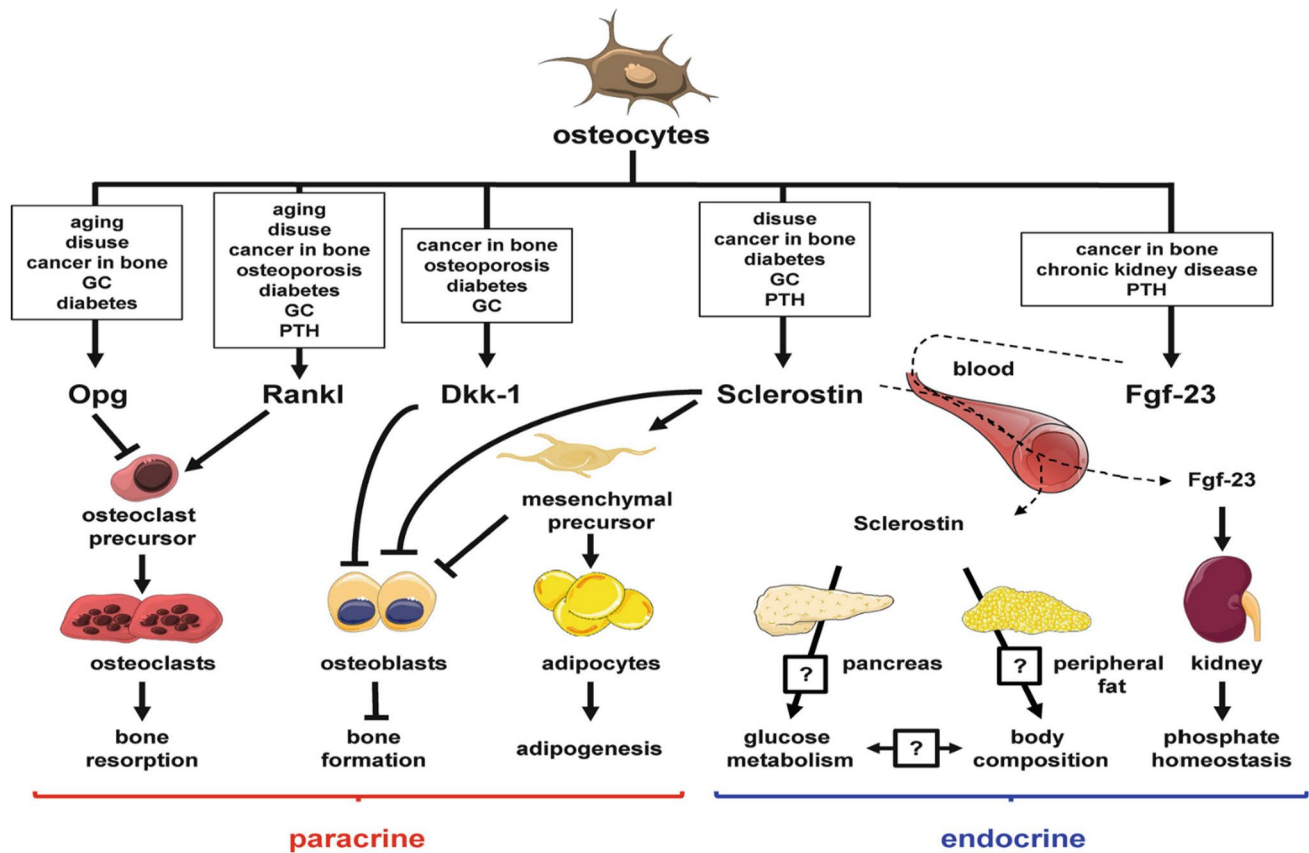


Fig. 4 Basic Aspects of Osteocyte Function [9]

and mechanoenzyme. In the second step, the focal adhesion protein complex, and its various actin-associated proteins, such as paxillin, vinculin, talin, and zyxin, as well as osteocyte cytoskeleton components, are involved. In response to mechanical stimulation, osteocytes emit a variety of secondary messengers, including ATP, Nitric Oxide (NO), Ca^{2+} , and prostaglandins, which alter bone physiology (PGE2 and PGI2). Whatever method is employed, keep in mind that osteocyte mechanosensitive activity is feasible due to the large channel network that allows bone cells to communicate with one another [16]. Osteoclasts are cells that disintegrate (resorb) bone during normal bone remodeling as well as in pathologic situations that increase bone resorption [17]. Adult osteoclast stem cells originate in hematopoietic tissue [18]. A primary positive regulator of osteoclast formation, RANKL/TRANSC/OPGL/ODF is produced by bone marrow stromal cells and osteoblasts and is membrane bound and soluble [10]. Acid secretion and proteolysis are two processes that cause bone resorption at the resorbed edge on the apical side of the osteoclasts. Bone resorption is initiated by active proton secretion by a vacuolar type of ATPase (V-ATPase) and passive chloride transfer via a chloride channel. The inorganic matrix of the bones is dissolved by the hydrochloric acid secretion. Osteopetrosis causes A3

deficiency because the active osteoclastic V-ATPase contains an $\alpha 3$ subunit [11].

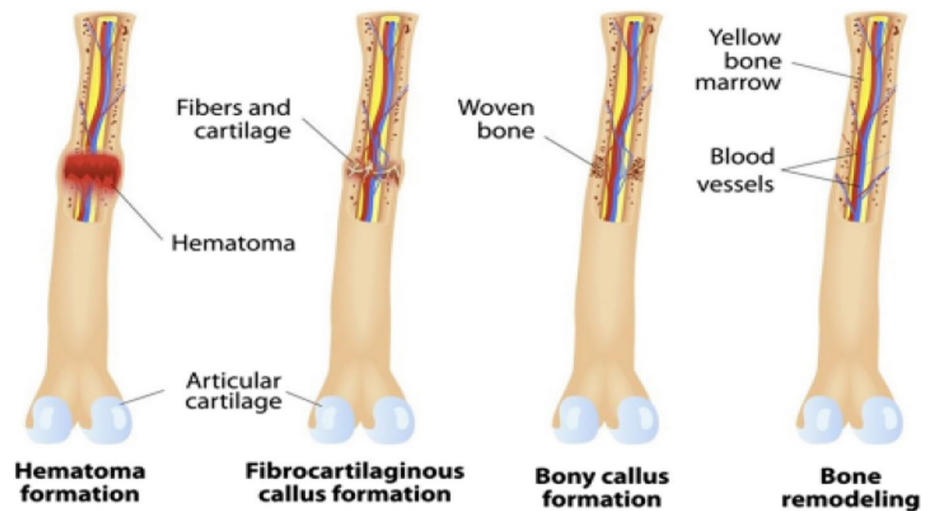
Bone Repair Mechanisms

A fracture is a break in the bone cortex's structural continuity that causes damage to the soft tissues around it. Fig. 5 illustrates the four steps of secondary healing after a fracture.:

- The development of a hematoma.
- fibrocartilaginous callus formation.
- The development of a bony callus.
- Bone reconstruction.

In up to 10% of all fractures, comminution, infection, malignancy, and altered vascular supply can all cause failure or delay in healing. Several factors influence fracture healing, which can be divided into two categories: local and systemic. Excessive movement, improper alignment, severe injury, and soft tissues in the fracture ends can all cause delayed or uneven mobility. Infection can result in sluggish, delayed, or uncoordinated healing. Blood supply—If there is a lack of blood supply to the fracture site, the blood supply may be delayed or unionised. Advanced age failure manifests

Fig. 5 Bone fracture repair and remodeling stages [12]



itself in the form of diabetes, parathyroid disease, and menopause endocrinology [12].

Each stage of the healing process starts with the formation of a hematoma in the inflammatory stage, which is caused by the disruption of a blood vessel after an injury or a bone fracture [13]. Within the first four days after trauma, the fracture hematoma develops osteogenic potential, allowing bone growth in ectopic places when explanted and, as a result, secondary fracture repair. Mesenchymal, endothelial, and immunological cells that enter the hematoma become embedded and produce the extracellular matrix cell (MSC), which then transforms into granulation tissue, before the soft callus forms. Cells and matrix are inextricably linked; cells command their matrix, while the matrix provides the environment in which signals directing cellular processes such as proliferation, differentiation, and migration are transmitted. The surrounding tissues, particularly the bone marrow, provide factors or cells that infiltrate the wounded bone region [14]. This stage starts the moment the fracture occurs. During a fracture, the blood vessels supplying the bone and periosteum break, resulting in the formation of a hematoma around the fracture site. The hematoma clots, paving the way for short-term healing. Pro-inflammatory cytokines such as tumor necrosis factor-alpha (TNF-), bone morphogenetic proteins (BMPs), and interleukins are released when a bone is broken (IL-1, IL-6, IL-11, IL-23). These cytokines attract macrophages, monocytes, and lymphocytes to the site, where they improve crucial cellular function. These cells work together to remove damaged or necrotic tissue and to produce cytokines such as vascular endothelial growth factor (VEGF) [19]. A fibrocartilage callus is a transient fibroblast and chondroblast development that occurs around a bone fracture while the bone tries to mend itself. The cells gradually disperse and go inactive, laying inert in the extracellular matrix that becomes the new bone [20]. The release of VEGF stimulates angiogenesis and the granulating tissue

with fibrin begins to develop in the hematoma. There are more mesenchymal stem cells in the region, and they start to evolve into fibroblasts (driven by BMPs). This is an indication of chondrogenesis, with a fibrocartilaginous collagen-rich network covering the fracture ends and a hyaline cartilage sleeve around them. Around the periosteum layers, osteoprogenitor cells form a tissue layer [21]. The cartilaginous callus begins to ossify endochondrally. RANK-L is used to differentiate between chondroblasts, osteoblasts, and osteoclasts. As a result of the absorption, the knickknack begins to calcify. Despite this, braided bone is fixed sub-periodically. The newly created blood vessels continue to proliferate, allowing mesenchymal stem cells to differentiate. At the end of this phase, a solid calcified juvenile bone callus forms [22]. While osteoblasts and osteoclasts continue to migrate, the hard callus remodels repeatedly, a process known as "coupling remodeling." This 'coupled remodeling' is a delicate balance of osteoclast resorption and new osteoblast bone formation. Finally, a compact bone replaces the callus's center, while lamellar bone replaces the callus's edges. The vasculature also undergoes significant remodeling as a result of these changes. The process of bone remodeling takes several months and eventually leads to normal bone structure renewal [23].

Casting and Traction Non-Operative (Closed) Therapy (Skin and Skeletal Traction)

Casting: Any fractures that are displaced, shortened, or angulated must be minimized as much as possible. To immobilize the limb, splints and casts made of fiberglass or Paris plaster are utilized.

Traction: A treatment method for fractures and dislocations that cannot be healed with casting. Traction methods include Skin traction and skeleton traction that are the two types of traction methods. The process of attaching the

tapes to the skin of the limb beneath the fracture is known as skin traction. A pin is inserted into the distal bone to treat a skeletal tension fracture. To facilitate traction, the patient is placed on traction apparatus. For this pin, weights will be used. This technique is most used to treat thighbone fractures and surgical treatment. Internal and External Reduction (ORIF). This is a procedure that exposes the fracture site and reduces the fracture. Internal fixation is accomplished using intramedullary nails, cables, plates, and screws.

External fixation is a type of fracture treatment that involves stabilizing the fracture from a distance away from the site of the fracture. A preoccupation with what is going on in the outside world. It promotes bone length preservation as well as alignment without the use of a cast. External fixation is carried out in the following circumstances: Soft tissue burns and wounds, open soft tissue-engaged fractures, pelvic fragments Fractures that are both large and unstable Fractures with a lot of weak spots, Extending the time limit procedures, Fractures that are infected or do not heal [15].

Conventional Technologies for Bone Scaffold Fabrication

The treatment of bone fractures and the restoration of serious bone abnormalities are critical. A number of bone repair and transplanting replacements have been developed as material science and technology have progressed [16]. A broken bone cannot heal on its own in a variety of situations. The bone

defect may exceed the threshold dimension after significant traumatic bone loss or primary tumor removal, and mechanical fixation may not be enough to cure it. Additional material is required to fill in the gaps for such serious flaws. Autogenous bone transplantation is the current gold standard for treating these serious deformities. Self-generated bone grafts have three main properties: osteogenic, osteoinductive, and osteoconductive. The term "osteogenic" refers to the process of transforming living cells into osteoblasts. Osteoinductive refers to the ability of local or distant cells to differentiate into osteoblasts in order to improve bone healing. Bone grafts also act as scaffolds, allowing new bone to grow on their surface (osteoconductive) [17]. Several criteria have been established for the production of tissue engineering scaffolds. (1) The scaffold should contain appropriate-sized interconnecting pores for tissue integration and vascularization; (2) it should be made of biodegradable or bioresorbable material so that tissue can eventually replace the scaffold; (3) it should have adequate cell-based surface chemical properties; (4) it should be mechanically suitable for the intended implantation and managing site; and (5) should not produce undesirable cellular adhesion reactions; and (6) should be conveniently manufactured in a variety of shapes and sizes [18]. Several methods for converting synthetic and natural scaffolding into porous structures have been developed. Scaffolds with a continuous porosity structure but no micro-architecture for long-range channelling are produced using traditional scaffold manufacturing procedures. Fig. 6 depicts the various approaches, and this section examines

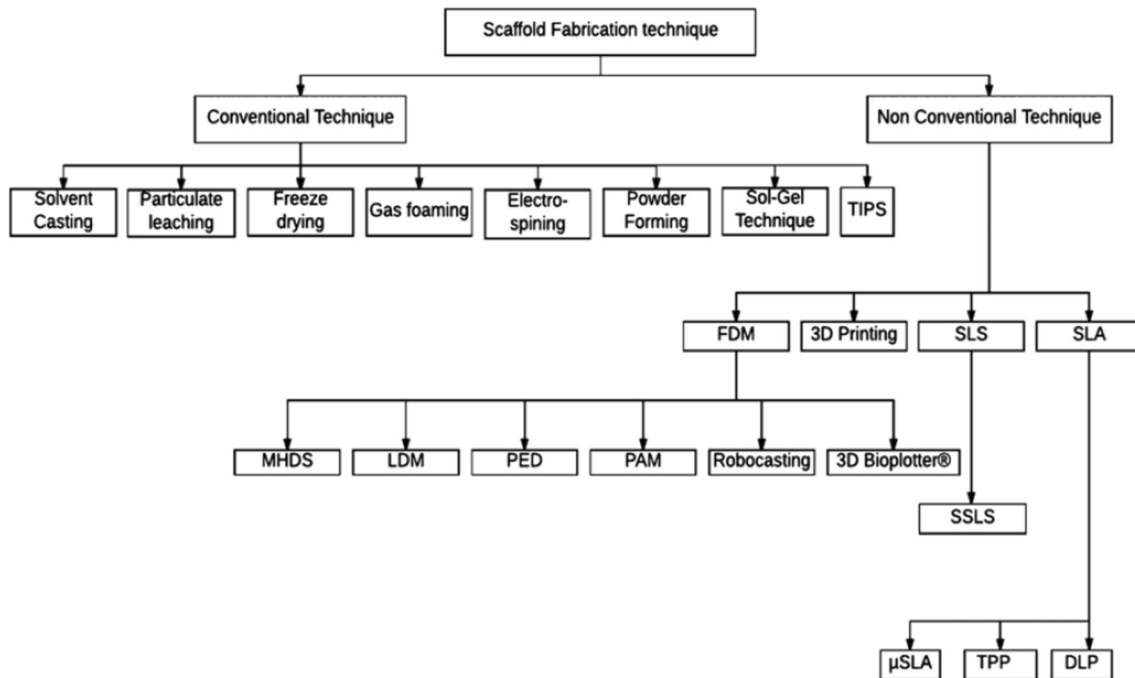


Fig. 6 Various scaffold fabrication techniques [24]

and explains the complexities of various traditional and additive manufacturing technologies [24].

Solvent Casting and Leaching of Particles

The method involves dissolving the polymer solution in a solvent containing uniformly distributed salt particles of a specific size. An evaporation of a salt-particle matrix takes place. The salt leaches into the porous structure after the matrix is submerged. The solvent-coated liquid particle coating can only be applied to thin, three-dimensional membranes of thin wall specimens; otherwise, the soluble particles cannot be separated from the polymer matrix. This method enables the creation of scaffolds with a permeability of 50–90%. [25]. Four steps consist of the solvent casting/salt laundering technique: (1) homogeneously dispersed porogenic particles into polymer solution; (2) the resultant mixture is dissolved into the mold; (3) the solvent is disposed from the solution through evaporation; and (4) the polymer/salt composite is immersed in water, or a suitable solvent to release porogenic particles. A variety of salts have been employed as porogen agents, including sodium chloride (NaCl), sodium bicarbonate, sodium acetate and saccharose [26]. SCPL (solvent casting particulate leaching) is a simple and straightforward procedure. Mikos et al. invented it in 1999. To address the drawbacks of the fiber binding technology, a SCPL was created. In this approach, the seven salt portions were disseminated in the PLLA/chloroform solution and plugged into a glass container. The salt particles' chloroform was insoluble. The solvent might evaporate, and vacuum drying eliminated any remaining residue [27]. Because it is easy to handle and easily available, salt is the most commonly used particle. For example, gelatin particles promote adhesion and proliferation. SOO WON SUH et al. investigated the biocompatibility of two scaffolds made of salt (salt scaffold) or gelatine (gelatine scaffold) in this work. The sieved salt and gelatine particles (with particle sizes ranging from 100 to 180 micro-meter) were distributed in a poly-lactic coglycolic acid (PLGA)/chloroform solution and cast in a teflon container. The solvent can evaporate, and vacuum drying eliminates any remaining amounts. By immersion into warm water (40 °C), the particles were allowed to leach away. Cultivated chondrocytes and bladder muscle cells (knee cartilage) were grown on every scaffold (5*106/cm²) and cultivated for three weeks, with hematoxylin and eosin stain being measured for their proliferation. These results indicated a superior cell adhesion at the beginning stage of the gelatin scaffold and a substantially greater proliferation of cells for 3 months in both cell types. The improvement in the efficiency of a gelatin scaffold also helped make the pores more porous [28]. N. F. Mohd Nasir et al. investigated the feasibility of fabricating bone tissue scaffolds utilizing a mix of Trong clay and hydroxyapatite

(HA). Weighted and mixed ratios of Trong clay, HA, and sodium chloride as the pyrogen were 9:1, 8:2, 7:3, 6:4, and 5:5. Using distilled water, a slurry of Trong clay-HA mixes was created, and then, sodium chloride was added to the solution. The liquids were put into Teflon molds and then incubated at 65 °C for around 48 h. After that, the freshly created samples were submerged in a 25% glutaraldehyde solution for 5 h to cross-link both strong clay and HA. This procedure was continued for approximately 4 days after the immersion of the samples for salt leaching in the distilled water, and this should contribute to the pore formation of bone tissue scaffolds. Trong clay-HA mixes were observed as a potential material for manufacture of bone tissue scaffold, and the best observed ratio was 9:1 with 90 wt% Trong clay and 10wt% HA. Scaffolds were, however, unable to maintain their structural integrity when all the samples produced by the technology and the proportion were dissolved within a mere 1 h. The 9:1 Trong clay-HA ratio maintained a scaffold structure integrity, manufactured by means of indirect 3D printing after 388 °C heat treatment and according to FESEM analysis results, the pore size was around 500 µm, and the indirect 3D printing method is thus suggested as a promising technique for creating a 3D bone scaffold made of Trong clay-HA composites [29]. To manufacture porous PLA scaffold with an axial porous size grade, a progressive solvent casting/porogen leaching process (PSC/PL) was developed (Xinghou Gong et al.). Fig. 7 shows how a graded macro-porous PLA scaffold was gradually produced in a Buchner funnel utilizing a Vacuum Pump to permit solvent removal. The weight ratio of PLA to NaCl was kept constant at 1:9 in multiple casting layers to achieve 90 percent porosity with graded pore size. To make the casting solution, 0.33 g PLA was dissolved in two ml of chloroform (CHCl₃) and then, equally sprinkled NaCl with the required size into the solution. By lowering the dimension of NaCl, 13 casting solutions were utilized to create the graded macroporous PLA scaffold; the casting solution was mixed to make a pasty mixture for 3 min. Buchner then moved the pasty to a funnel (50 mm inner diameter). The combination was then volatilized under a vacuum pressure of 0.08 MPa, and the pressures were released as the mixture's color changed to white. The Buchner funnel was then refilled with a new casting solution, and the preceding operations were repeated until the necessary structures were constructed. After the disinfectant was fully removed by vacuum, salt leaching was collected from the scaffold and air-dried for 24 h at 30 °C before being vacuum dried (1 mmHg). To avoid damage, all samples were stored in a desiccator until characterization, and the results demonstrate that as pore size rises, the compressive moduli of the PLA scaffolds decrease [19]. When characterized using a scanning electron microscope, NaCl-based 6.6 composite scaffolds of (nanohydroxyapatite)/nylon show composite powders with variable n-HA contents and

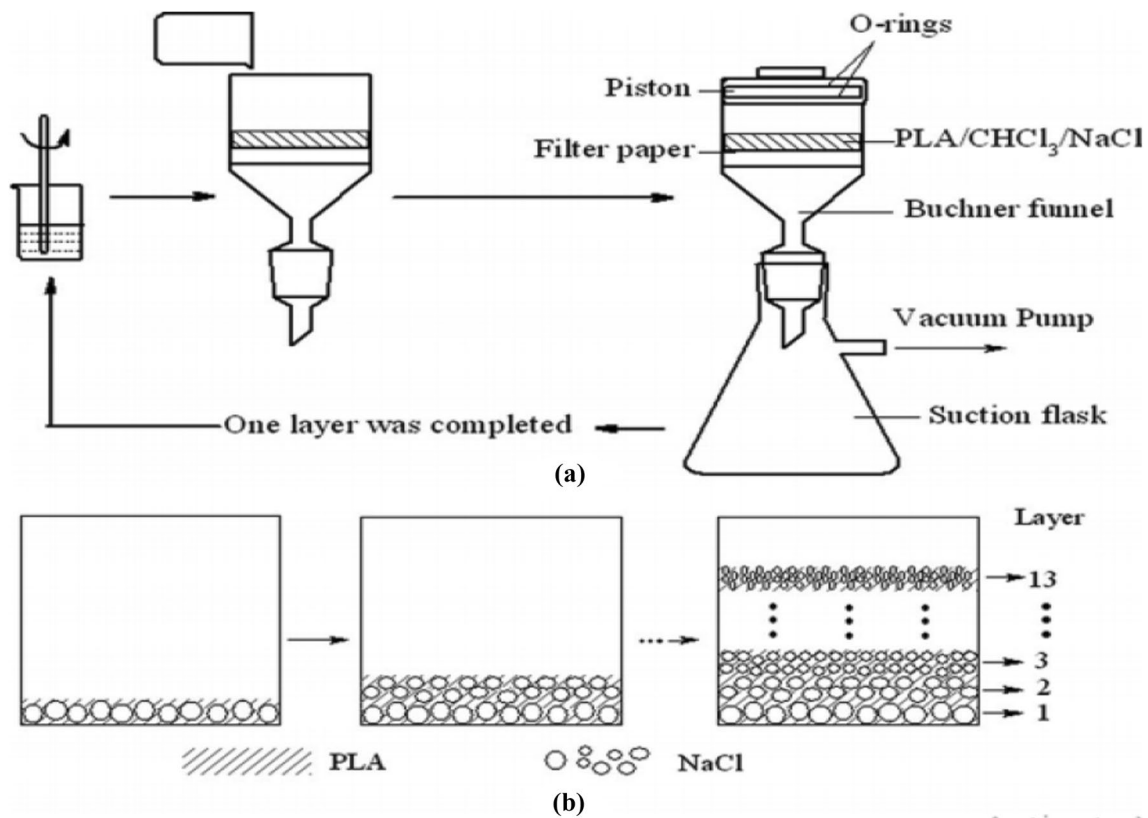


Fig. 7 The fabrication process is depicted in this diagram, which includes **a** the apparatus and **b** the PSC/PL method [19]

compound microstructures with interconnected porosity and approximate optimum pores of about 200–500 micro-m, as well as a higher level of apatite formation on the scaffold surface [30].

Freeze Drying Method

Freeze-drying is a process that removes residual solvent from a substance, resulting in a dry powder that is easy to load into a cell. In solvents, the substance is frozen in a dry icy bath. The solvent is vaporized and vacuumed away, leaving a dry powder behind. The temperature is kept low enough during freezing to prevent the phase-separated polymer solution from being remixed. There are numerous benefits to using freeze drying as a drying method:

- Low-temperature drying prevents heat-sensitive items' deterioration.
- The fluid can be dosed with precision.
- During the process, it is possible to adjust the humidity content of the final product.
- The dry product is physically attractive.
- The dried product is promptly reconstituted with a high specific surface.

The freezing-drying method scheme shown in Fig. 8 has been used in tissue regeneration research to create scaffolds made of polymers like PLLA [21].

Silk has been boiled for 1 h in a Na_2CO_3 aqueous solution of 0.5 wt percent and washed with water fully to remove sericin proteins. The de-composite silk (mole ratio, 1/8/2) at 80 °C has been dissolved at $\text{CaCl}_2/\text{H}_2\text{O}/\text{CH}_3\text{CH}_2\text{OH}$. Fibroin solution was then filtered and dialyzed for 3 days to create and concentrate the fibroin solution at 50–55 °C with stirring yields of 4 wt percent fibroin solutions, 6 wt percent, 8 wt percent and 12 wt percent (Qiang Lv et.al) in the refrigerator at –20 °C every 12 h. Then, ice and soil chemicals were freeze and a porous matrix remained. The crystallization and insolubility into water was induced into methanol for about 1 h after the drying porous matrices were created. The insoluble fibroin three-dimensional scaffolds are formed when methanol has evaporated at ambient temperature [31]. Dissolving 5 g of sodium alginate in 100 mL of distilled water at 2 h(h) at 50 °C in magnetic stripe at 2 wt percent acetic acid formed a bio-nano-compound porous cylindrical bone scapula by dissolving 5 g of cylindrical bone scaffold. After that, high-energy ball milling is used to generate powder diopside ($\text{CaMgSi}_2\text{O}_6$) (HEBM). For 20 min, a particular amount of dissolved sodium alginate and diopside bio-ceramic is blended using an IKA mechanical

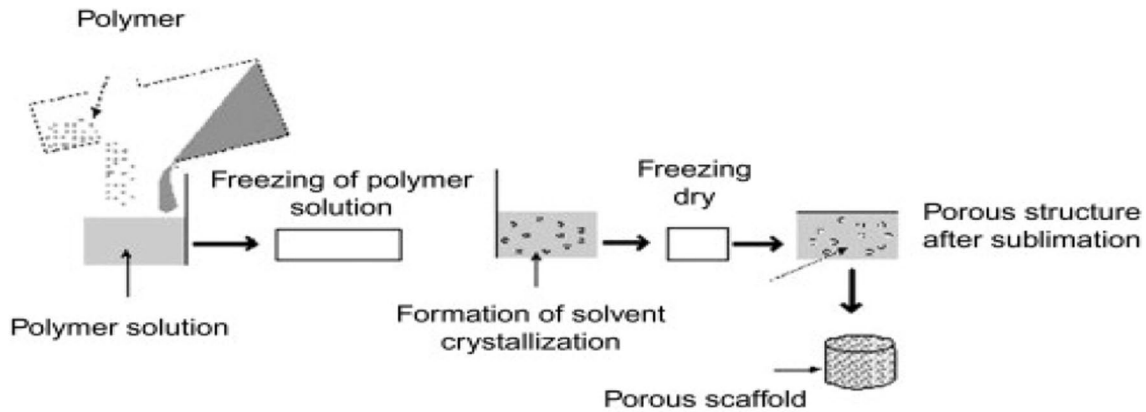


Fig. 8 The freeze-drying systematic approach to fabricate scaffold [21]

mixer. Following that, different concentrations of magnetite nanoparticles (0 wt%, 5 wt%, 10 wt%, and 15 wt%) are mixed with the Na-Alginate-Diopside solution at ambient temperature and then, frozen for 24 h at 65 °C. Using a high-energy ball mill, celecoxib is doped into the structure of MNPs. The porous bio-nanocomposite is then taken out of the refrigerator and freeze-dried for 24 h at temperatures below –45 °C [32].

Gas Foaming Method

The gas-foaming method involves placing a substance, usually polymeric, in a chamber with a gas, such as CO₂, and gradually increasing the pressure until the gas is soluble in the polymeric solid phase. As a result, the polymer is effectively saturated with gas. When the pressure is reduced to atmospheric pressure, the gaseous phase becomes thermodynamically unstable. The gas begins to phase separate from the polymer, and the gas molecules cluster together to reduce free energy, resulting in the formation of pores. Gas molecules diffusing to the pore nuclei cause the pores to enlarge. The resulting structure is very porous, but mostly is closed-porous, as gas between pores is rapidly depleted. Each time the approach is utilized. Pore training does not occur in a predictable way. This technology has been integrated with the salt-leaching method to establish greater interconnection between pores in the gas-foaming procedure. This procedure was paired with the salt-leaching process. The hybrid approach starts by making a porogen-polymer composite. After that, the composite is placed in a high-pressure atmosphere with a gas to allow the polymer and gas to combine. After that, the pressure is reduced to ambient, and the gas molecules generate pores within the structure. Finally, the scaffold is immersed in deionized water (or another solvent) to dissolve the porogen particle, resulting in the formation of more pores and improved pore interconnectivity [22]. Polyurethane foam manufacture is an example of gas foaming in

industry. When water is introduced to the reaction mixture, it combines with the isocyanate group to generate an a carbamic acid derivative, which decarboxylates to carbon dioxide. Because pore diameters are difficult to control and the typical pore diameter is too high (500–1000 micro-meter) to allow optimal cell proliferation, this approach is rarely used for scaffold creation. As a result, gas foamed polyurethane scaffolds have mostly been used for bone regeneration. The apparatus used in the foam manufacturing process is depicted in Fig. 9 (top row). A single cylindrical reactor with a thermostatic and necked neck makes up this system. An aqueous solution containing biopolymer, surfactant, and one of the gas-evolving pair's reagents is poured into the reactor. To keep the solution constantly mixed, a mechanical stirrer is used. The other reagent in the gas-evolving pair is added to the primary solution through the lateral neck, causing gas and foam to form. After the foam has stopped expanding, stir for a few minutes to achieve greater homogeneity and a narrower bubble size dispersion [33].

The following step is to accelerate the solidification of the moisture after its synthesis in order to avoid instability. This can be achieved by either exploiting biopolymers such as gelatin, which gels quickly, when exposed to low temperatures, for natural thermal gelling. If biopolymers are not gel, the liquid foam can be frozen at 280 °C, or, after being placed in a suitable vessel, in a vapor atmosphere of nitrogen that is liquid. This rapidly vitrifies the continuous phase of the foam preventing any phenomena of spray instability [23]. In a later phase, a chemical cross-linking technique can be used to improve the scaffold's mechanical stability and resistance in the cell culture media. Because the amount of gas produced by the reaction, which is mostly contained in moisture, is difficult to control and dose, this technique is used to create inhomogeneous topologies with uncontrolled and unpredictable pore sizes and reduced inter-pore connections. This results in a wide range of hole sizes and interconnections in the morphology of the resulting fatigue [34].

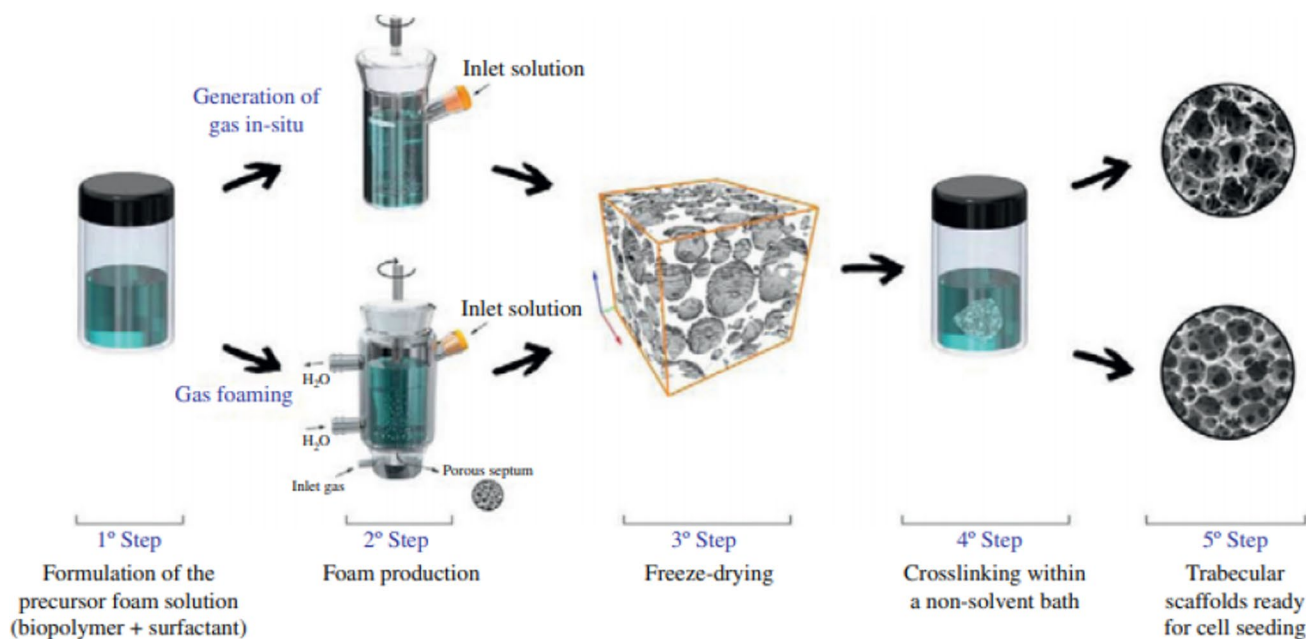


Fig. 9 This graphic depicts the equipment and experimental methods required in the fabrication of scaffolds employing chemical (top row) and physical blowing (bottom row) gas [33]

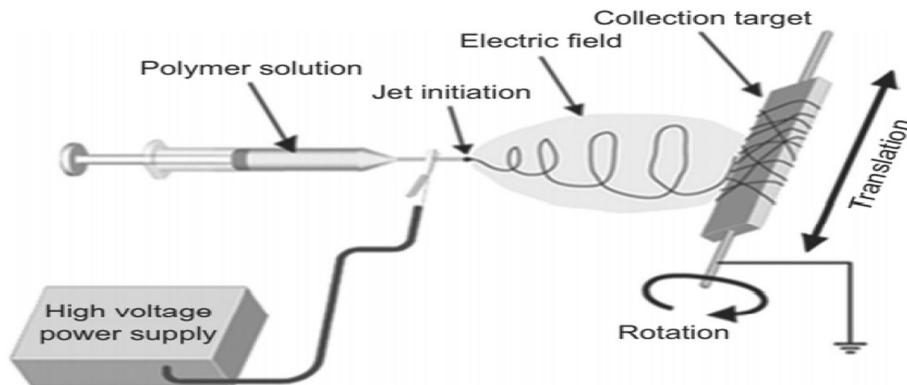
Electrospinning Method

Electrospinning is a single scaffold manufacturing technology that creates a Porous, Three-Dimensional Scaffold in the extracellular matrix. Electrospinning is a popular method for producing nanoscale (1000 nm) and micro-scale (0.1 μm) fibers. The initial step in electrospinning, A high potential is applied to the syringe as the solution is pressed through it with a syringe pump in electrospinning. As the charged solution escapes the needle, a "taylor cone" forms where the electrostatic repulsion is powerful enough to cause a fine stream of solution to erupt from the needle. The solvent evaporates during flight, and the charge migrates to the surface of the forming fiber. Because of the electrostatic repulsion felt over small bends, the fiber whips around. The introduction of an electro-field creates

a repulsion of mutual charge in the polymer solution or melt, which directly opposes the surface tension of the polymer solution. The charge disruption overcomes the surface voltage to generate a jet when the intensity of the electric field is raised. Finally, as the jet travels to the collector, the ejected polymer solution and melt oppose one another, and the solvent evaporates, forming fibers. Finally, the fiber is collected on a grounded plate, or in the case of aligned fibers, separated collecting plates or a spinning mandrel or disk as shown in Fig. 10 [35, 36]. Electrospinning is done in a controlled environment at ambient temperature.

The electrospinning process for polymer melts must be carried out under vacuum. There are four distinct zones in the electrospinning process, according to most experts:

Fig. 10 In academics, this is a typical electrospinning arrangement [36]



- (1) The base region: the solution’s charged surface at the nozzle end,
- (2) The jet region: here is when the solution follows a straight path.
- (3) The splay region: this is where the jets break into many nanofibers.
- (4) The collector zone: this is where the nanofibers will eventually settle [37].

The constraints of RP techniques for producing tiny size fibers and electrospinning for controlling fiber deposition prompted the creation of an. Electrospinning-based rapid prototyping (ESRP) is a process that uses electrospinning to create prototypes. This ESRP approach combines rapid prototyping with electrospinning to give RP the capacity to build a repeatable pattern and electrospinning the capacity to make a continuous fine fiber. For layer construction, this approach uses the RP process of FDM, but instead of employing the extrusion process to create fibers, electrospinning is used to generate electrostatic force to draw a continuous fiber from a liquid solution. The fiber is put down at predetermined positions from a nozzle to a collector to produce patterns layer by layer and observed that due to the presence of a machine vibration that affected the diameter of fiber, straight and gap size the manufacturing procedure was replicable and reproducible, and the three lay-down patterns were distinct. The stack of layers can be produced with higher precision if the vibration is reduced, and the solidification is regulated. The machine may be used not only to produce woven fiber cloth but also to produce non-woven scaffolds. This makes it possible to

make scaffolds on a single machine with alternating layers of woven and unwoven layers [38].

Powder Forming/Powder Metallurgy Method

Powder sintering, a conventional powder metallurgy process, has been frequently employed to create porous materials for scaffolds due to its ease of usage. Metal powder particles are compressed and sintered using this process. The interstices of powder particle configurations generate porous structures. As a result, the pore sizes and shapes of sintered powder compacts are determined by the sizes and shapes of the beginning powder particles, with a maximum porosity of 35 percent. To achieve larger porosity levels and better control over porous structure in scaffolds, powder sintering can be combined with the space holder approach [39]. Powders can be sculpted or engineered to fit into molds or dies, then compacted under pressure to form shapes. The schematic representations for several of the powder producing processes are shown in Fig. 11 a and b. Simple or sophisticated compacted shapes are possible. The compacted portion is frequently porous, necessitating a post-forming heat treatment step called sintering to make a dense final part. Polymer granules can also be molded into a variety of shapes. Rotational molding is used to transform these particles into complicated, hollow structures. Fig. 11c illustrates this point. Finally, powders are used in a variety of additive techniques. One of these procedures, selective laser sintering, is depicted in Fig. 11d [40].

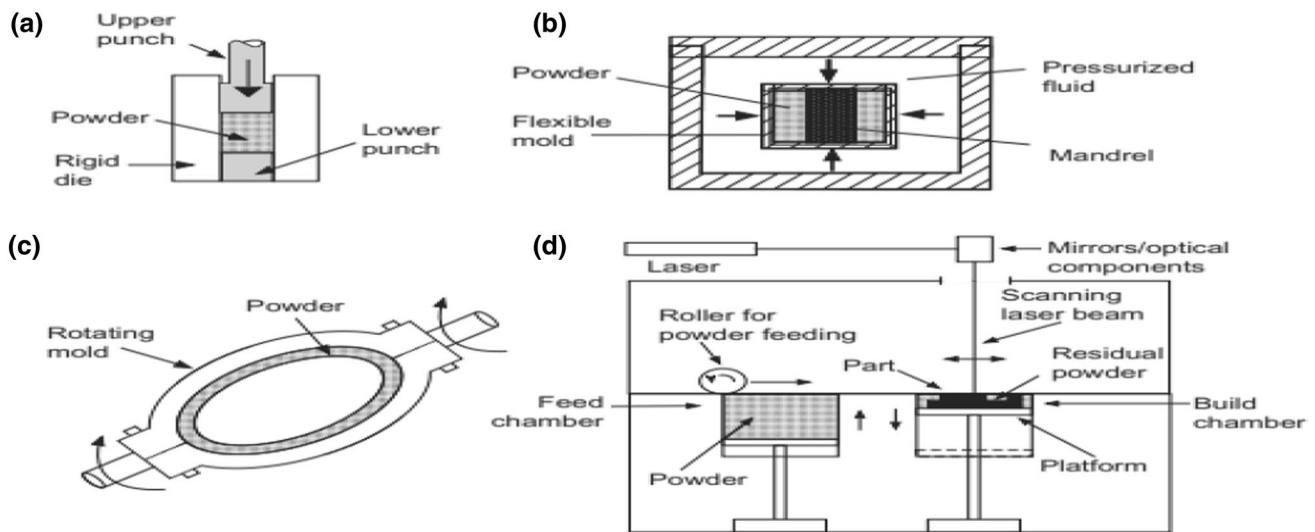


Fig. 11 In the following diagrams, powder forming processes are shown: **a** uniaxial—compacted powder into a green part using a punching and stiff die; **b** isostatic compaction—compacted powder into a green part using a pressure mold, flexible mold and rigid man-

drel; **c** rotary pulp—powder is distributed into a rotating mold, heated to create a melted layer to form it; **d** selective laser sintering—powder is dispersed on a platform and converted to solid through laser beam scanning layer by layer [40]

Sol–Gel Method

The sol–gel technique is thought to be effective in changing the surface of substrates. The ability to achieve a large area and stable surfaces is the most significant benefit of the sol–gel technique. The chemical and physical properties of the materials produced by the sol–gel process are influenced by the experimental conditions. There are two primary reactions in the sol–gel process: (1) hydrolysis of precursors in acidic or basic conditions, and (2) polycondensation of hydrolyzed products [27]. The concept of a sol–gel method is the synthesis via controlled hydrolysis and polycondensation of the homogenous solution from its original components. The soil is placed on the material surface, converted into a gel, and eventually heat treated into a layer of oxide. At higher temperatures of hot treatment, the oxide layer is nonporous and glassy or crystalline. It remains amorphous and porous at lower heat treatment temperatures. The scaffolds are created by dissolving inorganic metal salts or organic metal compounds in a solvent, resulting in the formation of a colloidal suspension (sol) via a series of hydrolysis and poly-personic reactions; after casting the sol into the mold, wet gel is formed and converted into dense ceramic or glass items via further drying and thermal treatment (Fig. 12), Sol–gel technology’s advantages can be leveraged to create biological sensors, laser materials, and delayed drug administration. High raw material costs, significant degradation of processing time, persistent fine pores, hydroxyl and carbon, and health hazards from the extended propensity to organic solutions are among the drawbacks [41]. It has been reported that the Carbon nanotube (CNT)-reinforced functionally graded bioactive glass scaffolds fabricated by the sol–gel method and dip-coated with the polymer polycaprolactone (PCL) have enhanced the compressive strength of the additively manufactured scaffolds by 98% [42, 43].

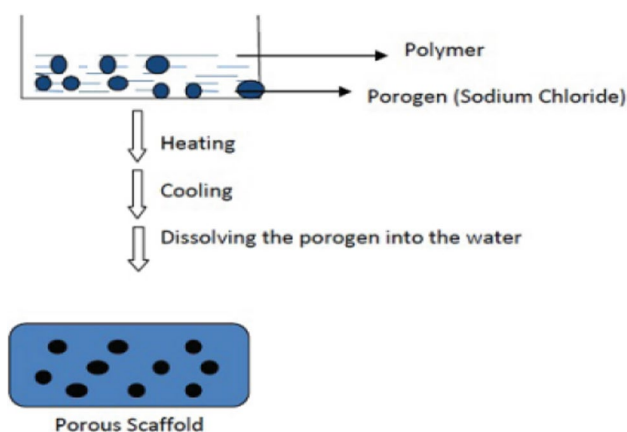


Fig. 12 Scaffold manufacture employing the technology of sol–gel [41]

Thermal-Induced Phase Separation (TIPS) Method

TIPS is a low-temperature method designed to force phase separation via the temperature alternate related to setting the homogeneous polymer solution with a high temperature in a decrease temperature environment to induce phase separation so that a polymer-rich phase, as well as a poor polymer phase, is achieved. A control over several variables, including polymer and solvent types, polymer concentration and temperature for phase separation enables the development of a range of scaffold topologies [44]. The main benefit of this procedure is that the settings are adjusted to attain a high porosity. The application of thermal phase separation (TIPS) and the freezing dryness has been found to yield porosity > 95 percent of scaffolds. The pore size of the scaffolds can be controlled by the size of porogen used. The porosity and pore size of the scaffold can also be controlled by varying the amount and size of the salt particles, respectively [45]. Table 1 shows the various conventional methods with its drawbacks and applications [46].

Non-Conventional Technologies for Bone Scaffold Fabrication

Scaffold manufacturing can include solid free-form manufacturing (SFF) technologies which produced three-dimensional structures of complicated geometry using layer-by-layer stacking of 2-dimensional (2D) patterns [47]. SFF is an integrated production, computer-aided and automation technology. The merging of the manufacturing of scaffolds and SFF thus offers various advantages. First of all, numerous technologies are implemented for the production of scaffolds, such as computer-aided design (CAD), computer-assisted fabrication (CAM), and computed tomography (CT). This enables the creation and manufacture of a scaffold with complicated geometry or a tight form tolerance that cannot be created in a typical manufacturing environment. Second, CAD, CAM and CT are essential components of a production (manufacturing) environment with computer aid, meaning it is possible to automate and better define the full rebuilding or repair of a damaged tissue by employing a scaffold. Third, the scaffold manufacture could be subject to a variety of SFF technologies such as three-dimensional (3DP), stereo-lithography (SL) and fused deposition modeling (FDM). Finally, for manufacturing miniature components the manufacturing resolution of the SFF techniques can be enhanced. This allows SFF to create advanced scaffolds with complicated geometry and micro-scale functions. SFF technologies can therefore play a critical role in the production, including pore size, porosity and distribution, of unique exterior forms and specified and replicable internal morphology. In addition, the mass transfer across the fabric

Table 1 Factors, disadvantages, and applications of scaffold fabrication methods [46]

Methods	Unique factors	Drawbacks	Applications
Solvent casting/salt leaching Method	Controlled porous biodegradable scaffold	Residual solvents and porogenic materials, limited mechanical properties	Tissue Engineering of Bone and Cartilage
Ice particle leaching method	Pore structure control and thicker scaffold generation	Mechanical properties are limited, and pore interconnectivity is poor	Bone tissue engineering with porous 3D scaffolds
Gas foaming/salt leaching method	Sponge with controlled porosity and pore structure	Mechanical properties are limited, and pore interconnectivity is poor	Tissue engineering and drug delivery
Solvent evaporation technique	Because of the larger surface area, high-density cell culture is possible	Low mechanical strength due to pore interconnectivity	Repairing bones
Freeze drying method	Durable and flexible 3D porous sponge structure	Pore size is small, and the processing time is long	Scaffolds with complexities
Thermally induced phase separation	For cellular transplantation, a porous scaffold is used	Scaffold morphology is difficult to manage accurately	Complex tissue engineering forms
Nano fiber electrospinning process	Biomechanical, high surface area	The major challenge with electrospinning technique is cell seeding. Limited mechanical property decreased pore size with thickness of fiber	Drug administration, wound treatment, synthetic skin, soft tissue, and yarn
Sponge replication method	Porous ceramic scaffold interconnected	Pore interconnectivity is insufficient	Bone tissue engineering
Melt-based rapid prototyping process	Mechanical strength of a complex 3D solid object	Only a few types of polymers are available, and the equipment is quite expensive	Hard-tissue scaffold, honeycomb structure scaffold

of oxygen and nutrients can be considered at the design stage by use of the geometry design parameter [48]. Table 2 indicates the various non-conventional method to fabricate the scaffold and its advantages and disadvantages [39].

Melt–Dissolution Deposition Technique

Fused Deposition Modeling (FDM)

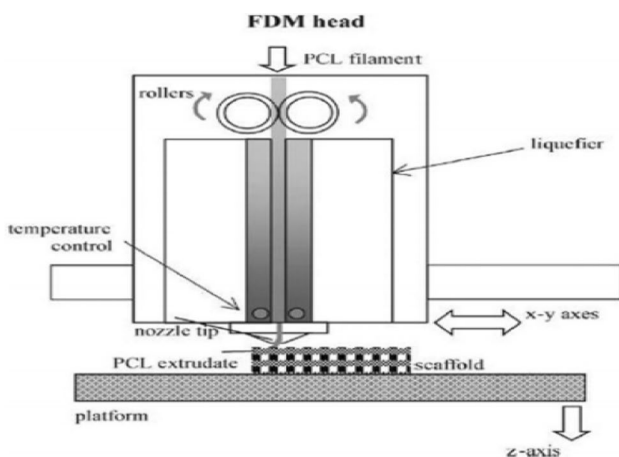
The FDM process makes use of and distributes two materials as depicted in Fig. 13: one for the component and one for the disposable support structure. The material is a plastic roll on a spool. To make one object, a filamentthe feedstock material is heated and fed into a semi-liquid condition in a temperature-controlled extrusion head. The material is extruded and precisely raised in ultra-thin layers by the head on a fasten-free basis. The dust has a programmed mechanism for turning on and off the melted substance. The previous layer’s enhanced lamination results in a 3D plastic model formed on a single strand. On the axes x, y, and z, the system draws one layer of the model at a time. The filament is formed in the shape of a narrow ribbon and ensures filament connection on each layer [49, 49].

The extruded filament that is placed on the platform is referred to as a "road." When another layer of road is laid on

the platform, one road quickly solidifies. The road that was previously deposited and layered by the latter road is referred to as a substratum. Overhanging geometries require structures to be produced automatically and then broken away from the item [51]. The loading of a model’s STL file into preprocessing software is the first step in FDM. The software divides the 3D model into tiny layers. Automatically inserted process parameters such as tip size, material type, and cutting speed result in the generation of a machine control file, Fig. 14 shows data processing in the FDM [52]. This horizontally oriented model has a mathematical division of 0.127 to 0.331 mm. While to dispense model and support materials, two different nozzles are employed. The support material (SR30-XL) in the Stratasys uPrint-SE system is water-soluble, while the model material (P430XL) is not. By exposing the FDM-prototyped part (which includes the model and support materials) to water, the final product can be readily separated. To alleviate prototype structural stress and warping due by the filament cooling phase, prototyping is done in a warm environment (about 72 0C). Plasticizers were used in four composite samples consisting of a plasticized blend of poly(3-hydroxybutyrate), amorphous poly(d,l-lactide), (n-Butyryl tri-n-hexyl citrate), and Syncroflex TM 3114. As a bioactive filler, a tricalcium phosphate blend (TCP = 7 percent, TCP = 93 percent, abbr. TCP) was

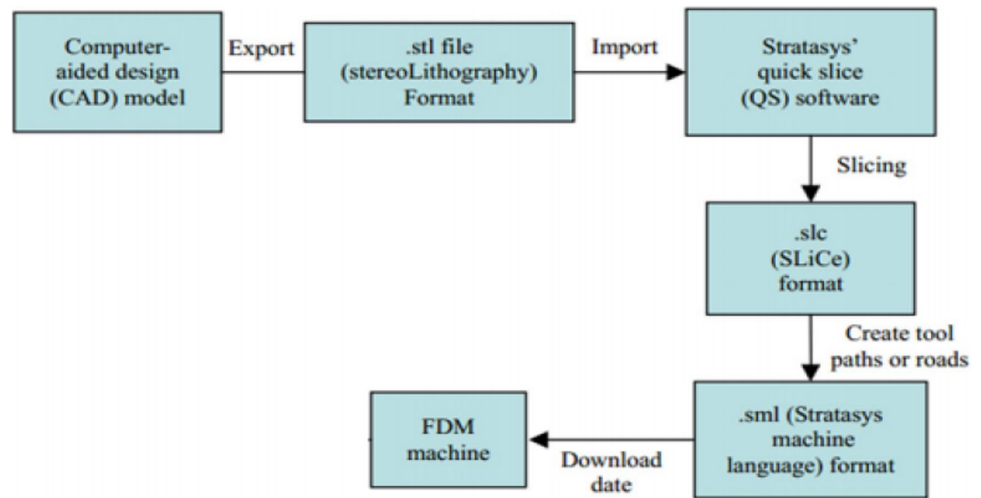
Table 2 Non-conventional scaffold manufacturing technologies classification [39]

Fabrication technique	Advantages	Disadvantages
<i>Non-conventional technologies</i>		
Stereolithography (SLA)	<ol style="list-style-type: none"> 1. Facilitates the elimination of waste in subtractive production methods 2. High-quality images 3. Pore interconnectedness that is consistent 	<ol style="list-style-type: none"> 1. Has photopolymerization limitations 2. Requires high quantities of monomers to induce monomer conversion and post-polymerization therapy
Selective laser sintering (SLS)	<ol style="list-style-type: none"> 1. Use ultra-high molecular weight polyethylene 2. The user has excellent control over the microstructure of the scaffold created by altering SLS process variables. 3. Used to achieve the desired qualities of the scaffold that was developed 	<ol style="list-style-type: none"> 1. More steps shall be taken to remove injected powder following the rotation of the phase 2. The temperature is high for operations
Solvent-based extrusion free forming (SEF)	<ol style="list-style-type: none"> 1. Can be utilized for the fabrication of composite products, including ceramic, metal and metal/ceramic 2. Can be utilized directly or indirectly for the printing of the real part or mold 3. It is a technology that can be utilized to precisely monitor the scaffold structure at the nano-level for revolutionary tissue engineering 4. Successful monitoring of the natural tissue structure as well as of the mechanical characteristics of the ground is necessary 	<ol style="list-style-type: none"> 1. Their design comprises changes in elements affecting the pressure of the extruder, including a ratio of the length to diameter of the nozzle, paste formulation and speed of the extruder
Bioprinting	<ol style="list-style-type: none"> 1. Low cost. 1 2. Enhanced accuracy and form complexity 3. High printing speed capable of maintaining high cell viability in parallel (80/90 percent) 	<ol style="list-style-type: none"> 1. It is a function of cell existence
Fused deposition modeling (FDM)	<ol style="list-style-type: none"> 1. Useful in the design of the scaffold in various ways 2. Low-temperature deposition 	Has restrictions on the use of biodegradable polymers

**Fig. 13** FDM Schematic [49]

applied to the matrix. The corotating meshing twin screw extruder was used to compound all the samples. Each sample for extrusion weighed 500 grams overall. The composite samples were heated twice, from 10 to 195 degrees Celsius, at a rate of 10 degrees Celsius per minute. All the tests were carried out in a nitrogen-rich environment. The polymer

sample weights were around 10 mg. 3D printing filaments were made from the composite granules prepared in the first phase. First, the filament was dragged into a 60-degree water tank. Second, the filament was directed to the draw-off device with the calibration unit to maintain a constant 1.75 mm filament diameter and the scaffold was created with an (FDM) original Prusa i3 MK3 3D printer. This printer has a maximum print space of $250 = 210$ per 200 mm, $x = y = z$; axes x and y are 10 microns and z axis are 5 microns in resolution. The Citroflex-based plasticizer has a very good softening effect at the cost of poor printability and inadequate performance during biological testing, according to scaffold characterization results from differential scanning calorimetry and tensile studies. In comparison with commercial polylactide filament, the samples with Syncroflex had a lower warping tendency, with a one-third reduced warping coefficient. Furthermore, the Syncroflex-based samples were non-cytotoxic and showed good biocompatibility [53]. Singh (2014) examined the surface quality of a hip joint manufactured utilizing a mix of FDM and IC as a case study. An ABS-based sacrificial design was created using FDM, and IC was performed with SS-316L utilizing different slurry layers, slurry viscosity, and primary layer drying time. The number of slurry layers, slurry viscosity,

Fig. 14 FDM data processing [52]

and main layer drying time all contributed 41, 32, and 25% to the surface finish of the implants, respectively, according to the study's findings. Singh (2015) conducted a similar type of experiment; however, the sacrificial models in this endeavor were composed of three materials (i.e., wax, ABS, and ABS coated with wax). Hip joint castings employing a wax pattern have been demonstrated to be more difficult than others. In 2016, Kumar et al. discovered that the volume/surface ratio and shell mold wall thickness had a significant (95% confidence level) effect on the surface durability of hip articulations [52].

Low-Temperature Deposition Manufacturing (LDM)

The production of the Low-Temperature Deposition (LDM), also known as quick freeze prototyping or freeze-form extrusion fabrication, is based not only on a quick deposition technique, but also on a separation phase procedure [53]. In addition to the controlled macropore size, LDM manufactured fabric scaffolds have interconnected micropores in the lines deposited. More crucially, the technique is green, which utilizes non-heating material liquefied. It has been used to create tissue designed scaffolds for the regeneration of bone, cartilage, blood vessels, and nerve tissue. It is a promising technique in the manufacture of fabric scaffolds that are similar to ideal and intricate organ design [54]. LDM is used to layer a scaffold in a low temperature chamber on a platform at a temperature below 0 °C, as shown in Fig. 15, and the scaffold is subsequently frozen for frozen solvent removal. LDM is a more durable scaffolding technology than fused deposition (FDM) and selective laser sintering. Its non-heating feature retains the bioactivity of the materials. A software-designed electrical model should, first and foremost, be faultless. The ground's shape and architecture are determined. Second, when polymeric materials are dissolved in solvent at greater concentrations, the scaffold

micropores shrink and the microphone wall thickens. Third, the LDM device's settings should be adjusted for the creation of fine scaffolds. The chamber is generally constructed at around – 10 °C to ensure that the extruded material is frozen during the forming process. The nozzle temperature should be significantly higher than the chamber temperature to allow the extruded lines to mix with the preceding layer. If the nozzle temperature is too low, the extruded lines will separate from the prior layer [55]. LDM with a pneumatic-extrusion-based feeding system and valve-control with a quick pressure/relief system can avoid the impact of over-accumulation on molding precision in the LDM process. As a result, tissue engineering scaffolds manufactured using a pneumatic-valve control process have precise dimensions and a wide spectrum of materials that can be used [56].

The inability to dissolve the polymers due to a lack of solvent is a serious issue. Because the forming temperature of LDM is below 0 °C, it is difficult to find more suitable solvents that can not only dissolve the polymers but also swiftly freeze in the forming chamber. So far, just a few solvents have been employed, including DIO, water, and diluted acid. As a result, it is challenging to obtain a homogeneous solution comprising both natural and synthetic polymers [54, 56]. Dixit et al. studied the effect of CNTs on compressive strength of bioactive glass (BG-B30). The inclusion of CNTs enhanced the compressive strength and induced surface roughness at the scaffold's surface led to better cell adhesion [57]. Table 3 gives the comparison of various methods for bone scaffold fabrication based on Melt–dissolution deposition techniques [58].

Selective Vacuum Manufacturing (SVM)

SVM is an RP approach that was developed to produce prototypes layer by layer using sandcasting and powder sintering techniques. Rather than using a physical pattern

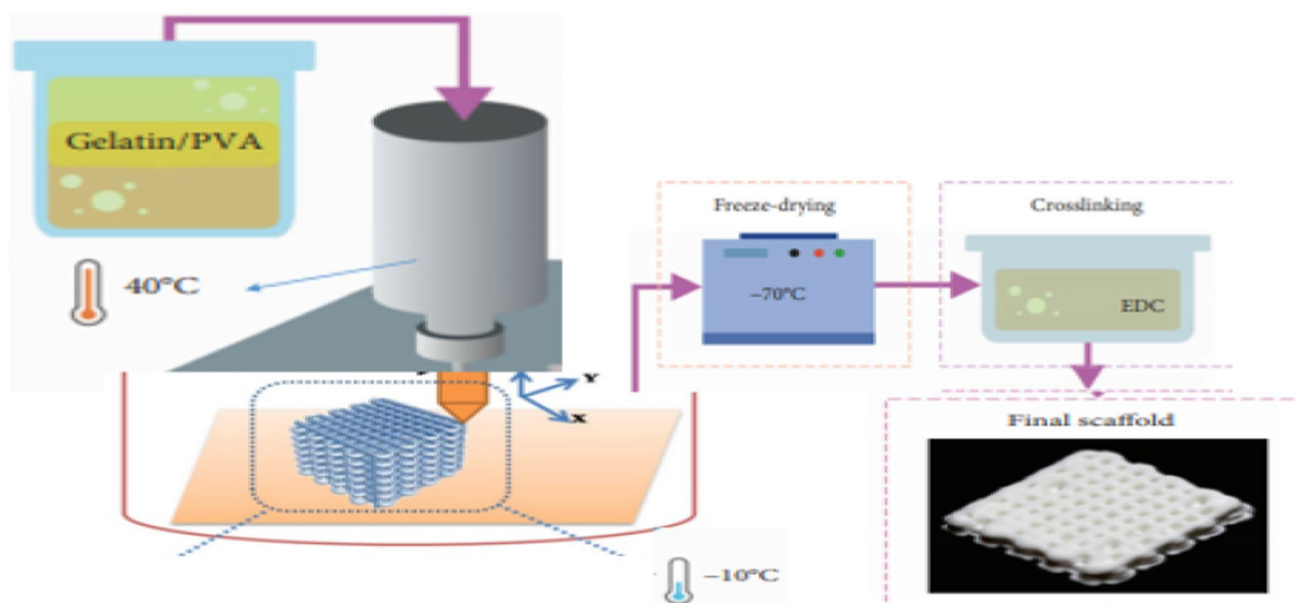


Fig. 15 Materials are extruded onto a low-temperature building plate during the LDM process for scaffold fabrication [55]

and material, vacuum pressures are used to create a desired cavity in which the powder material is placed and synthesized to build a cross section of the 3D prototype, resulting in a sand-casting prototype. Figure 16 depicts the stages of the SVM process. 1. Preparation of the supporting material bed; 2. vacuum cell laying; 3. filling of the formed cavity with the component material and 4. sintering in a solid layer. The whole prototype can be manufactured step by step by repeating these easy processes [59]. Koomsap P. et al. used poly-lactic acid, or PLA, as a scaffold material. PLA pellets were pulverized before use in the SVM process by spraying PLA solution into a water medium, then air-drying and gently crushing the powder, and the feasibility of using SVM was assessed using scaffolds with three different lay-down patterns (solid, 0/90, and zigzag). A LabVIEW program, which includes (1) vacuum head movement and filler movement, (2) motion for the heating and scraper unit, and (3) movement for the storage and filler platform unit, was drafted to control the movement of unit on the SVM machine. For the evaluation of the produced scaffolds, three types of tests were performed: scanning electron microscopy (SEM), porosity analysis, and mechanical tests. The experiment revealed that all created scaffolds, including solid scaffolds with no macro-porosity due to the lay-down patterns, had extremely high porosity. The high porosity, on the other hand, comes at the expense of low mechanical strength. Increasing the heating power to extend the necking areas can help improve this mechanical feature; however, it will result in scaffold shrinking. More PLA powder can be added to counteract the shrinkage effect and in order to

construct micro-scale scaffolds, the SVM machine needs to be modified for practical use [60]

3D Fiber-Deposition Technique

In this approach, the feedstock material is in the form of pellets or granules that can be poured directly into the heated liquefier. For articulate tissue engineering applications, PEGT–PBT block copolymer scaffolds (poly(ethylene glycol)-terephthalate-poly(butylene terephthalate)) have been developed. The material flow can be regulated by applying pressure to the syringe. The five main components of this 3D deposition unit are depicted in Fig. 17: (1) a thermostatically controlled heating jacket; (2) a melt co-polymer dispensing unit comprised of a syringe and a tap; (3) a force-controlled plunger to control molten co-polymer flow; (4) a stepper engine driven x2y2z; and (5) a position controlling unit comprised of a molded co-polymer. Stepper motor controllers coupled to a computer running Software for designing fiber deposition pathways [61].

Precision Extruding Deposition (PED)

This technology's extruder contains an integrated heating unit that melts the feedstock material, removing the requirement for precursor filaments. PCL scaffolds with 250 μm pore sizes were produced.

As depicted in Fig. 18, a XYZ position system, a material extruder system, and a temperature control system are among the hardware components. The software component consists of a data processing application and a system

Table 3 Comparison of several techniques used in tissue engineering for Melt–dissolution deposition [58]

RP system	Resolution (mm)	Material	Strength	Weakness
<i>Melt–dissolution deposition technique</i>				
Fused deposition modeling	250	PCL ^a , PP-TCP, PCL-HA, PCL-TCP	Superior mechanical strength; lay-down design flexible	Maximum temp; filament material must be produced; restricted processing window;
3D fiber-deposition technique	250	PEGT-PBT	Input material comes in the shape of pellets, which cuts down on preparation time. Pelletized input material	High-temperature filament with a stiff structure;
Precision extruding deposition	250	PCL	Pelletized input material	High-temperature filament that is stiff
Precise extrusion manufacturing	200–500	PLLA-TCP	Biomolecules can be included	High-temperature filament that is stiff
Low-temperature deposition manufacturing	400	PLLA-TCP	A wider choice of materials can be employed; biomolecules can be used	It's made with a solvent, and it needs to be frozen before it can be utilized
Multi-nozzle deposition manufacturing	400	PLLA-TCP	A wider range of materials can be used; biomolecules can be included; and extremely fine resolution can be produced	It's made with a solvent, and it needs to be frozen before it can be utilized
Pressure-assisted microsyringe	10–600	PCL, PLLA	A wider selection of materials is available for use	Small nozzle prevents particle inclusion; limited range of printed viscosities; solvent is utilized
Robocasting	100–1000	Organic ink	It's possible to use a wider choice of materials; biomolecules can be incorporated	Ink characteristics must be precisely controlled
3D bioplotter	250	Hydrogel	A wider choice of materials can be employed; biomolecules can be used	Low mechanical strength; smooth surface; low precision; lengthy processing; careful control of material and medium parameters; new material calibration
Rapid prototyping robotic dispensing system	400–1000	Chitosanchitosan-HA	A wider choice of materials can be employed; biomolecules can be used	Material and medium qualities must be precisely controlled; freeze drying is required
SLA stereolithography	–	PEG, PEGDA, PPF, PCL, PDLA	Quick speed, great resolution, support materials easy to remove	Small selection of resin and polymers photosensitive
SLS: selective laser sintering	–	Polymers, ceramics (PCL, HA, TCP)	Wide range of materials, excellent mechanical resistance, high accuracy, high porosity	Powdered compounds that are difficult to remove
FDM: fused deposition modeling	–	Thermoplastic polymers and their composites	Easy to use, minimal cost, several lay-down models	Filamentous materials, moderate speed, high temperature, and a flat surface
3DF: 3D fiber deposition	–	Thermoplastic polymers and their composites, hydrogels	Simple operation, minimal cost, resources in pellet form, and a shorter preparation time	High temperature

Fig. 16 SVM procedure steps [59]

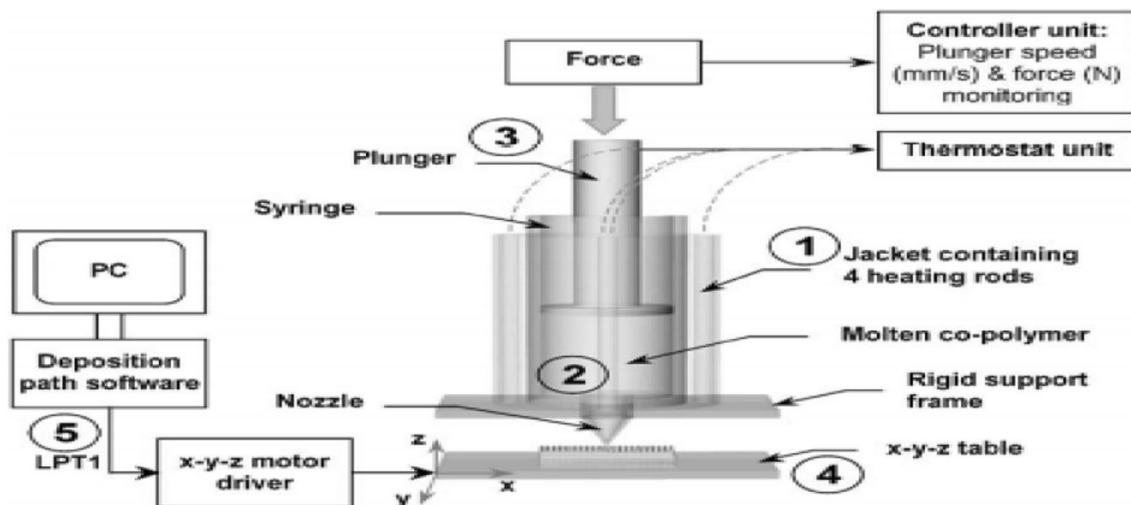
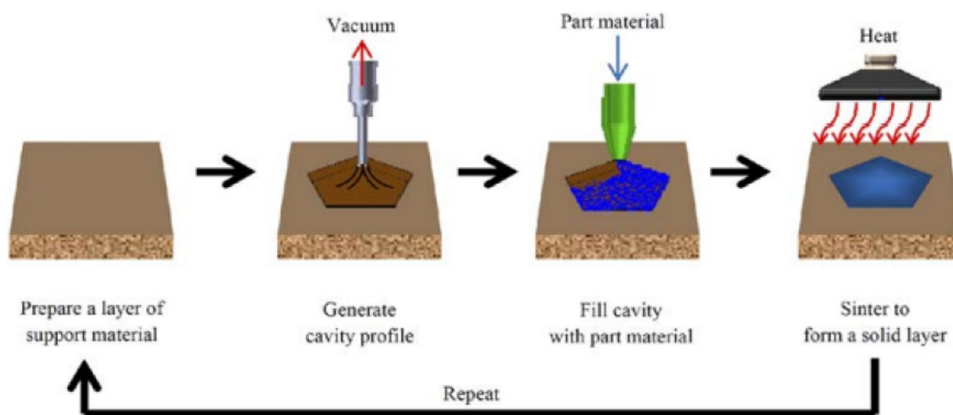


Fig. 17 Device for 3D deposition technique [61]

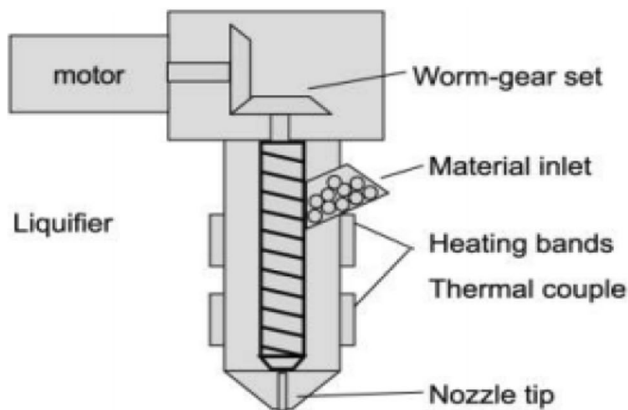


Fig. 18 A material mini-extruder schematic is shown in this diagram [62]

to the process toolpath to build a layered 3D object. The material mini-extruder system delivers the fused PCL to the deposition nozzle. The key distinction between PED and regular FDM processes is that scaffolding material can be directly put through the PED process without the need for filament preparation [62].

Pressure-Assisted Micro Syringe (PAM)

A Pressure-assisted micro-syringe (PAM) system is shown in Fig. 19. In this method, a micro-syringe is used to eject the polymer dissolved to the desired pattern at low and steady pressure. This method is resolution on a cellular scale, which in contrast to the previously disclosed techniques is very high. Vozi et al. have constructed 20 mm line-width PCL and PLLA scaffolds. The performance of this technology has been shown to be comparable to soft lithography. But very minute capillaries need to be handled carefully to avoid fracture of tips and high pressure is also required to get the material out of a small hole [63, 64].

control programmed. The data processing software builds the process toolpath after slicing the STL files. The system control software organizes material deposition according

Fig. 19 Schematic depiction of the mechanism of deposition controlled by pressures [64]

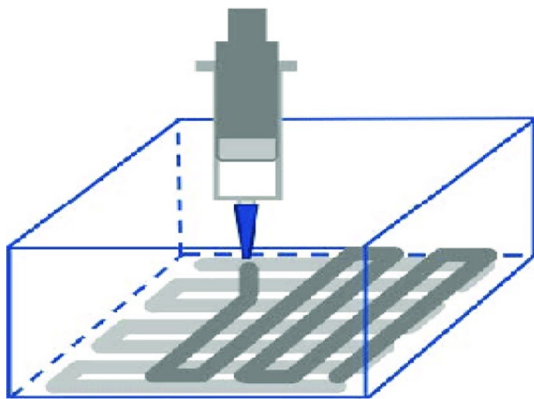
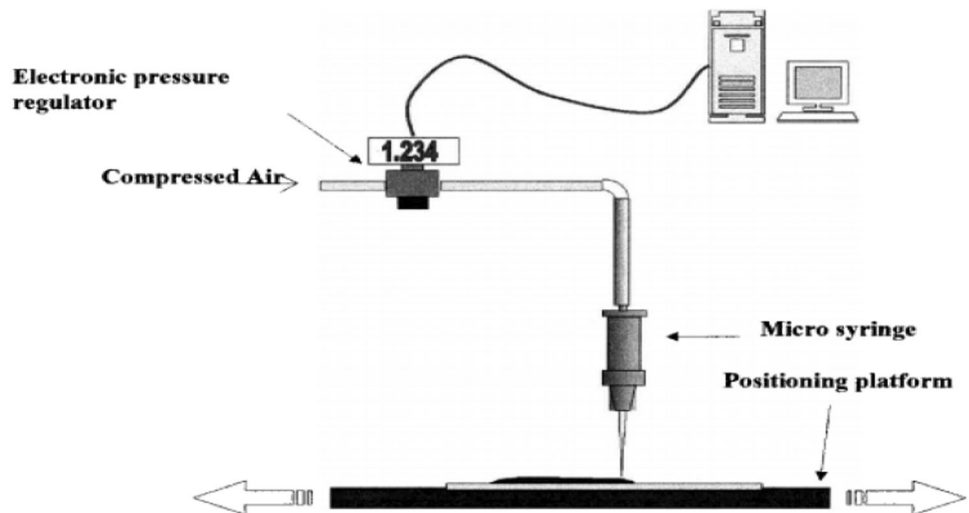


Fig. 20 Schematic illustration of the manufacturing process for robocasting. The ceramic scaffold is created from a CAD model layer by layer. The robot arm moves the injection syringe by means of the conical deposition tube and expresses the ceramic ink to form the desired structure immersed in an oil bath [65]

Robocasting

Robocasting is a manufacturing additive technology that allows scientists to produce scaffolding without the use of a sacrificial supporting material with concentrated colloidal suspension (ink/paste), with a minimum or no biological additive. The viscoelastic reaction in colloidal ink needs to be well monitored to ensure that the particulate system withstands compressible stress caused by capillary tension, thus retaining its shape over non-supported layers and no distortion of the subsequent layers. The arrangement of filaments in grid patterns creates three-dimensional macroporous channels as shown in Fig. 20. These routes can be accurately designed to form very homogenous macropores by changing the spacing and size of the rod. Micropores can be created by incorporating porogen in the suspension before extrusion, and it can produce extremely porous structures

(50–70 vol.%) with customized pores varying in size from a few hundred micro-meter's. A sufficient microspheres volume percentage is associated with microporosity. Finally, a temperature change in the sintering profile of the production tires can change the porosity of the sub-microphone [65].

3D Bio-Plotter

The 3D Bio Plotter System is a versatile, quick prototyping device mainly used to handle a wide spectrum in computer tissue engineering with biomaterials from 3D CAD models and CT data patients to a 3D physical scaffold as depicted in Fig. 21. It is also used to make ceramic paste components with a precision of up to 100 microlayers, as paste and gel material can be removed. The possibility to build hydrogel plots is probably the most attractive aspect of a 3D bio plotter. Simple structures like sheets, fibers, wovens and nonwovens can be created using gelatin, agar, fibrine and collage hydrogels. They are beneficial because they are flexible, structural like-matrix and oxygen and metabolite permeable [66]. A hydrogel acrylate poly(ethylene glycol) (PEG) with inkjet peptides was used for co-printing by Gao et al. Gao et al. Human MSCs were also found in the ultra-violet hydrogel, which resulted in simultaneous photopolymerization in hydrogel. With a cell viability of $87,9 \pm 5,3$ percent after 24 h of immersion, the finished fabric showed good biological compatibility [67].

Rapid Prototyping Robotic Dispensing System (RPBOD)

This system was created by Ang et al. and comprises of a computer-guided desktop robot and a single-component pneumatic dispenser. A small Teflon-lined nozzle was utilized to discharge liquid material into a dispensing media. In the preliminary investigation, chitosan scaffolds with pore diameters ranging from 400 to 1000 mm were constructed.

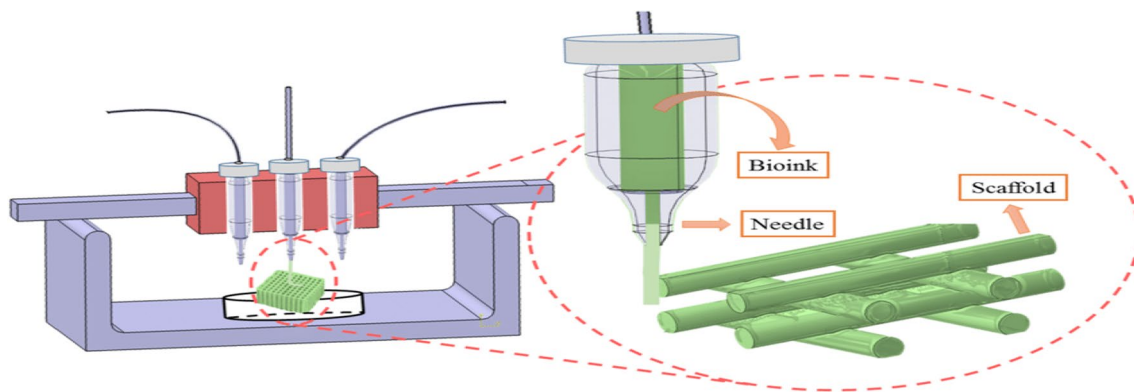


Fig. 21 3D Bio-plotter system outline [66]

To drive the dissolver through a small Teflon-filled nozzle into a dissolving liquid (sodium hydroxide–ethanol in a 7:3 ratio), a 30 mL barrel of dissolved hydroxyapatite (HA) in acetic acid was utilized. Using a pre-programmed lay-down pattern, the chitosan was built up layer by layer. The NaOH solution neutralizes the chitosan, resulting in gel-like precipitation with the cuboid remaining stable [68]

Particle-Bonding Techniques

During particle binding processes, particles are selectively connected to a thin layer of powder material. The thin 2D layers are connected to produce a complicated 3D solid. During the manufacturing process, it is supported and embedded in raw powder. As a result, this technology enables the creation of overlapping channels and structures. The item is taken from the bed of unbound powder once all layers have been completed [69]. Depending on the use, the powder used in a scaffold may be a pure powder or a coated surface powder. You can use a single powder or a combination of powders. These techniques can be utilized to develop porous materials capable of managing macroporosity and microporosity. Micro-porosity is created throughout the space by the granular powder. By altering the bonding area, this modulates pores. The pore size, on the other hand, is restricted to the size of the substance's powder. Prior to the bonding procedure, porogen mixing can result in bigger pores in the powder bed [70]. The powder components offer a rough surface to the scaffold. Topographic cues can have a significant impact on cell behaviors. When cells adhere to strain, stretch receptors are activated. Surface receptors on scaffolds can be twisted to variable degrees, resulting in cell-signal pathway activation. As a result, scaffolds constructed employing particle bond approaches may be preferable in the context of cell attachment [71]. [3D] Direct printing, fused deposition modeling, stereolithography, and selective laser sintering

are now employed to create 3D scaffolds using a layer-by-layer approach. Scaffolds ranging in size from centimeters to nanometers have been created using these approaches. It should also be noted that the terms "solid freeform manufacturing," "additive production," and "3D printing" have all become synonymous in the previous 10 years.

Direct 3D Printing

The process of constructing computer-assisted structures in consecutive layers is known as three-dimensional printing. Instead of paper, the 3D printer employs a liquid binding solution that is selectively applied to a powder bed. This procedure begins with a powder bed, which is placed on a building platform and, depending on the material, is equipped with a rolling mechanism. The printer nozzle then delivers the binder solution to powdery locations specified by the CAD. After the binder solution and powder have been mixed, the excess powder is removed (blown off). After the construction platform is lowered, a new powder coating is applied and flattened [72]. This procedure is repeated until the final structure is formed as shown in Fig. 22.

To broaden the range of 3D printable biomaterials, new methods for converting existing biomaterials for 3D printing into appropriate room-temperature formats must be developed. This is accomplished using solidifying fluid, non-brittle filament, laminated thin layers, and thin powder. For example, gelatin gel can be solidified by lowering the temperature, but the environment of low temperatures is incompatible with what is beneficial to cell survival, so a new mechanism of gelatin solidification, such as enzyme crosslinking solidification and the development of a new low-temperature hydride deposition mechanism for hydrogels and cells must be investigated [73].

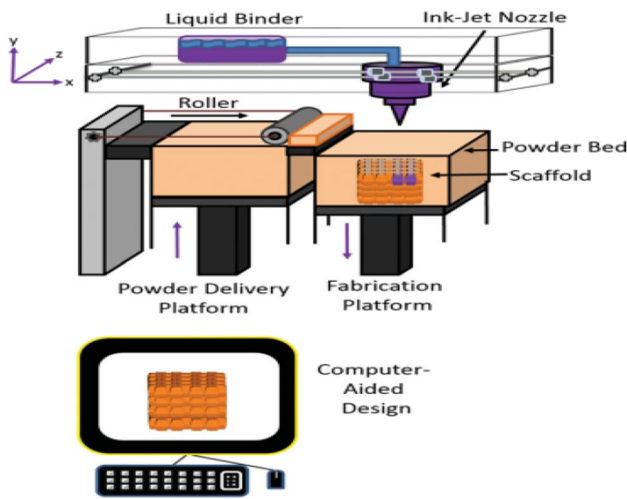


Fig. 22 A CAD scaffold is 3D printed directly, as shown in this diagram [72]

Selective Laser Sintering

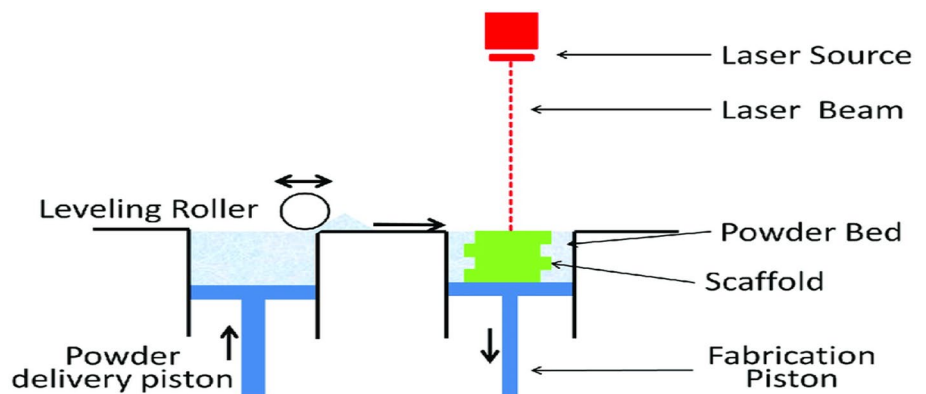
Selective laser sintering (SLS) is a quick prototyping technology used to generate powdered tissue engineering scaffolds. However, the typical scanning process generally results in struts of substantial thickness, which makes it quite difficult to build extremely porous and overall small scaffolds. Laser and powder synergy are critical to the SLS process, as well as laser preference is material dependent. Because of light-matter behavior, substances absorb light energy only at specific wavelengths focused on their optical characteristics. Generally, oxide ceramics poorly acquire in the approaching infrared range, whereas carbide ceramics absorb at 1.06 μm wavelength. Because of its good optical absorption characteristics, the CO₂ laser ($\lambda \approx 10.6 \mu\text{m}$) is best adapted for oxide ceramics, whereas the Nd:YAG, Yb:YAG, or Nd:YVO₄ ($\lambda \approx 1.6 \mu\text{m}$) lasers used in commercial selective laser melting machines are best adapted for metals and carbide ceramics. Regrettably, because of

its relatively small spot size for high dimensional accuracy, greater specific power, the YAG laser is frequently used in oxide ceramics. [74]. Selective laser sintering (SLS), as illustrated in Fig. 23, employs a high-performing carbon dioxide laser to fuse tiny polymers powder particles. The polymer PCL, calcium phosphates or polymer composites and bio-ceramic composites are the most typically employed materials in the SLS. In general, the manufacture of SLS ceramics is considered problematic because of the quick heating and cooling speeds generated by the high temperature laser which generates frequently weak scaffolds. The key advantage of SLS is its potential to produce highly detailed imprints with thin walls; however, its dimensional precision is only 150–180 μm in comparison with other AM processes. Additional SLS challenges include the inability to print growth factors and cells, as well as the reduction and bending of the scaffold due to thermal distortions. However, because of the high temperatures generated by the laser, natural polymers cannot be used in this process [75].

Stereolithography (SLA)

Stereolithography (SLA) is a rapid prototyping technology that uses photopolymerization to build three-dimensional (3D) scaffolds layer by layer from a computer-input design specification. This method enables the replication of scaffolds with controlled porosity, pore size, connectivity, and mechanical properties [76]. The photopolymerization method is a 3D printing technique in which light is gradually injected into ingredients (photopolymers, radiation-curing resins, and fluids) that are accumulated in layers in a bowl, resulting in a patterned 2D layer. These include stereolithography (SLA), digital light processing (DLP), and continuous direct lighting processing (CDLP). Furthermore, the SLA can be separated into two unique configurations based on the direction of the light source and the surface on which the photoactive resin is polymerized as (1) bath (free surface approach) and (2) bat (restricted surface method) as depicted in Fig. 24A and B. In the bath

Fig. 23 Selective laser sintering process (SLS) scheme. The top layer of powder on a powder bed is sintered/melted in a pre-defined design by a laser source. The powder bed is reduced in height, and a cool powder layer is placed above with a roller levelling. Then, the procedure is followed [74]



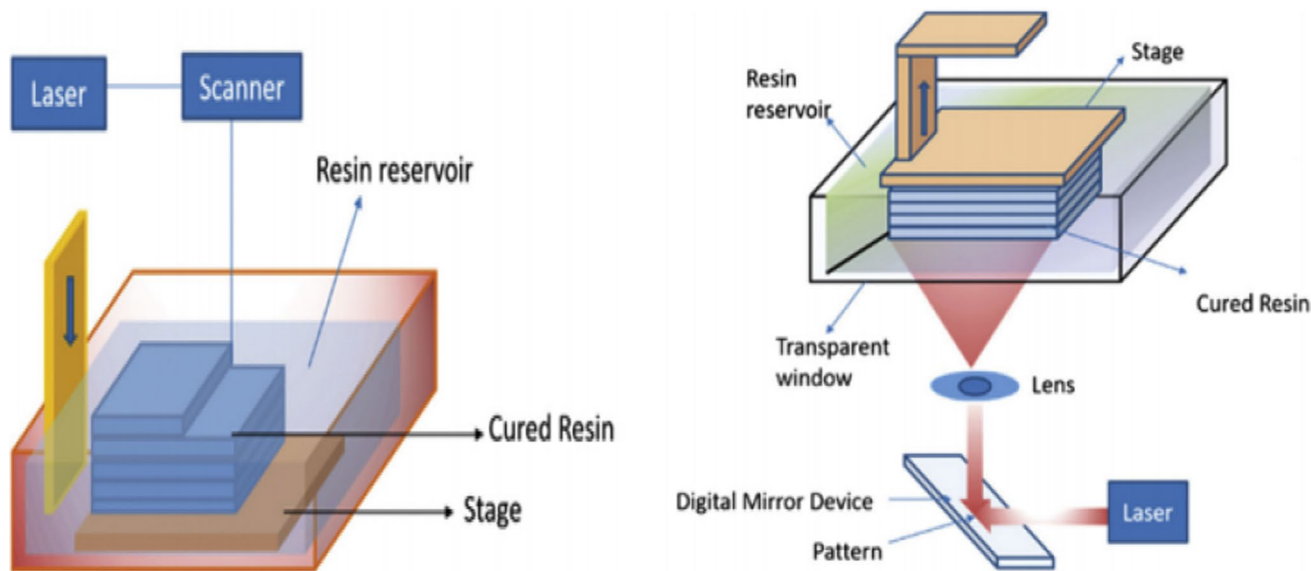


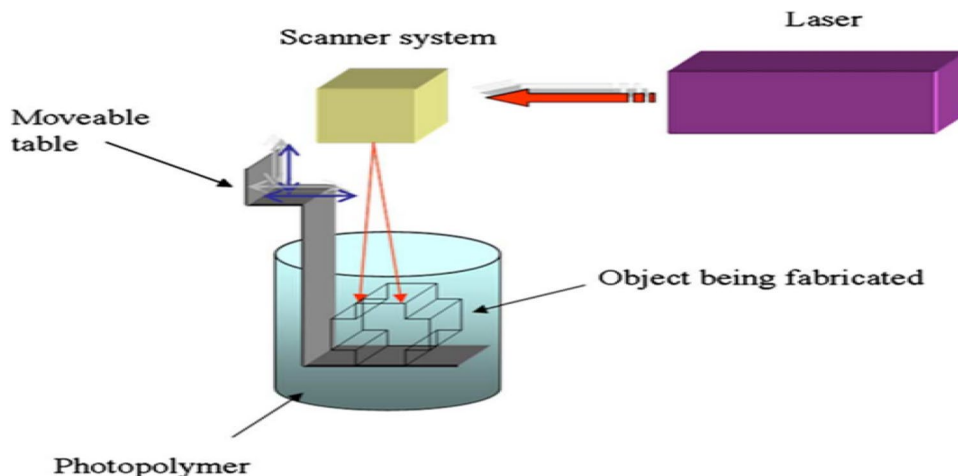
Fig. 24 Configuration of stereolithography (SLA): **A** bathing configuration and **B** bat settings (constrained surface approach) [77]

setup, the highest layer of the photoactive resin is polymerized by a line carrying the light source to the entire layer. Following the curing of the first layer, the substrate or phase is pushed down so that successive layers can be polymerized from the bottom up for effective 3D printing. In this technique, the thickness of the cured layer varies depending on the light source strength, scanning speed, depth of focus, and exposure period. A mask, which is a digital mirror device with a range of one million mirrors, can be employed in the bat configuration to cure the entire layer in one step. Furthermore, with such a system, the light source beneath the resin reservoir differs from the bath layout. The goal of this light source is to photopolymerize the thin fluid resin layer that occurs between the optically clear cup base and a moving substratum (stage) hanging above the cup. The stage is then elevated to allow

uncured resin to fill the space and remove the cured layer from the bottom surface of the vat as it prints [77].

Griffith and Halloran created ceramic parts using stereolithography (SLA) in 1996, utilizing a UV photocurable monomer loaded with alumina, silicon nitride, and silica particle suspensions as shown in Fig. 25. To cure the monomer, a UV laser beam guided by CAD cross-sectional data was used. The combining of the ceramic particles resulted in the formation of a green body. Pyrolysis was used to remove the polymer binder, and the ceramic components were sintered. The same method was used by Levy et al. to create hydroxyapatite (HA) scaffolds for orbital floor implants [78]. When used for selective laser sintering (SLS), the polymer absorbs infrared ($h = 10.6 \text{ m}$) radiation, causing the entire polymer particle to absorb volumetrically. To put it another way, each polymer particle is completely melted to form the

Fig. 25 A stereolithography (SLA) system is depicted in this diagram. A UV laser is utilized to reinforce the cross section of the model while leaving the other sections liquid. The table then compresses to allow for the application of another fluid resin layer to cover the solid polymer [78]



desired shape. Surface selective infrared sintering (SSLS) employs laser energy that is near-infrared ($\lambda = 0.97 \text{ m}$) and is not absorbed by polymer particles. To begin the sintering process, a small amount of carbon microparticles (0.1 wt%) is evenly distributed over the surfaces of polymer particles. As a result, the melting process is limited to the surface. Eugeni N. Antonov et al. demonstrated the application of the (SSLS) approach using a 0.97 m wavelength continuous wave (CW) diode laser by incorporating an enzyme of ribonuclease A into poly(D,L-lactic) acid (PLA) and assembling three-dimensional matrices at three different laser intensities. Following laser processing, assays of this model enzyme show that ribonuclease activity remains strong and, importantly, the polymer's molecular weight or Poly-dispersibility does not change [79].

RP's Tissue Engineering Challenges

Tissue engineering has the challenge of imitating a scenario *in vivo*. Engineered tissues like the kidney, liver, nerve, gut, pancreas, even the muscles of the cardiovascular and valves are being attempted. One of the problems of engineering cartilage or bone is to synthesize scaffolds which have acceptable mechanical properties. The implanted scaffold should be mechanically strong in these tissues, from the time it is implanted to the end of the restructuring process. Another problem is that age depends on the healing process. The healing pace for young people is fast, but the repair rate for elderly people slows down. Many materials with good mechanical characteristics lack high porosity and many materials which have proved to be *in vitro* might fail to be used *in vivo* because of insufficient vascularization capacity [80]. Thus, there are several hurdles to be addressed despite the growing interest among tissue engineers in the use of RP, i.e., the limited choice of materials, the appropriate design of the scaffold, the scaffolds' bioactivity, cell-seed, and vascularization problems. Each problem will be thoroughly discussed.

Material Range

The processing techniques used in RP treatments are extremely advanced. Every procedure requires a different type of input material, such as filament, powder, solid pellet, or solution. As a result, the scaffold materials selected must match the planned RP process and be easily created in the necessary form. The breakage profile and mechanical strength of the structure are further factors to consider when selecting materials. The degradation-absorption mechanism is influenced by several interdependencies, including polymer backbone hydrophilicity, crystallinity, the presence of catalysts, porosity volume, and the surface.

Everyone has the ability to gradually degrade the implant and send stress to the surrounding tissues at a rate sufficient to cure it. This is one of the most serious concerns in tissue technology development right now. Although biodegradable polymers are known to contain largely non-cytotoxic breakdown products, little is known about the acidic byproduct effect of the scaffold, which varies with degradation rate. Sung, H., et al. discovered that rapid polymer degradation had a negative impact on cell viability as well as *in vitro* and *in vivo* migration into the ground. This could be explained by the rapid local acidity generated by polymer breakdown. For the classification of the material degradation profile, a more systematic research technique is required. Cells can detect mechanical properties of the adhesion substratum with high sensitivity, allowing them to control the integrative binding of the focusing plate and the cytoskeleton. In the case of excessively rigid and non-deformable adhesion, the cells are unable to rearrange and recruit receptors into focal adhesion plaques, which is required for the generation of signals that ensure the viability of anchor cells. Similarly, the material is to conform due to its incapacity to withstand the traction forces induced by the cytoskeleton assembly, preventing cell anchoring [81].

Architecture Design of Scaffold

The various tissue characteristics demand varied optimum pores for different tissue types. Despite much evidence-of-concept studies showing that a variety of pore dimensions for distinct cell types exists optimally, nothing is known about the ideal pore sizes for certain cell types. The selected pores are therefore subject to general empirical recommendations [82]. RP-made grooves usually have several edges and grooves. These topographical discontinuities may influence cell adhesion and migration. Yin, L. et al. cultured cardiac cells on micro-grooved Elastic Scaffolds to investigate topographical changes in heart electromechanics. The railings have a depth of 50 mm and a width of 120 mm. The authors demonstrated that the microstructure has an immediate impact on heart function and is responsive to rhythms via calcium-dependent mechanisms [83]. The surface roughness of the scaffold is important in cell matrix interactions. The rough powder surface created by RP techniques based on powder can increase cell adhesion. If the surface is excessively rough, the cells that attach to these materials are unable to form independent focal adhesion plaques or bridge defects. Furthermore, surface roughness may cause actual injury to the cell. In other RP methods, such as the FDM and the bio plotter, the smooth surface of solidified materials cannot offer strong adherence to the cell, necessitating additional surface modification and coating [84].

RP-Manufactured Scaffold Bioactivity

Both structural and chemical signaling molecules control the cell's interaction with the scaffold, which is critical in cell adhesion and continued activity following initial contact. The degree of early cellular adhesion controls the number of focal plates generated, as well as their size, shape, and distribution on the cell membrane, which in turn determines the size and shape of the cell spread area. The breadth of the spread is crucial for future anchoring-dependent cell migration, proliferation, and differentiation. Controlling cell proliferation and other behaviors of advanced bio specific materials currently involves the modeling or incorporation of controlled releases of biomolecules such as natural growth factors, hormones, enzymes, or synthetic cell cycle regulators of the material surfaces via adhesive molecules. Some RP systems, such as the MDM and bio plotter, can integrate biomolecules during the cycle [85]. More information, however, is required to develop the most favorable scaffolds, such as the biomolecule, ideal concentration, and spatial management. Ca^{2+}

Seeding of Cells and Vascularization

The effective and consistent distribution of a high cell density throughout the scaffold volume is one important barrier in the tissue formation process. A Petri dish is the only technique of cell seed allowed by the Food and Drug Administration. This strategy, however, was shown to fail in the uniform distribution of cells deep within the scaffold [86]. Cellularization of a 3D scaffold is thus inextricably linked to advancements in bioreactor technology. Enough scaffolding is critical for maintaining proper perfusion in the architecture of large tissue structures. Integrating the growth factor into the scaffold is an alternative method for vascularization. Several angiogenic determinants were discovered, including vascular, endothelial, fibroblastic, epidermal, platelet-derived growth factors, and transformed growth factors that induce new vascular cells in tissue endothelial cells [87]. Endothelial cell transfer into the skull is an alternative strategy for increasing vascularity [88]. Experiments on rats revealed that endothelial cell transplantation can result in vascularization of matrices. In this approach, the bioactivity of the scaffold is crucial. To improve the success of grit-based tissue engineering, the RP approach provides the flexibility and capability to link the design and production of bioactive seed to improved cell seeding techniques.

New Areas of Rapid Growth of Prototyping: Automation and Direct Organ Production

Bioartificial organ production technologies are several enabling approaches based on bionic principles that can

be employed in human organ manufacturing. Significant progress has been achieved in the development of various organ production technologies over the previous ten years. Overall, organ manufacturing technique is classified into three categories based on automation level: (1) fully automated, (2) semi-automated, and (3) hand crafted (or hand-made) [89]. The ease of scaffolding using RP allows for a simple technique of analyzing the interaction between the cell and the matrix. Individual influences of material stiffness, topography, and roughness, as well as porpoise and structure, can be examined to acquire a better knowledge of cellular behaviors. Recent study has uncovered a new school of thought that uses layered production methods to manufacture an organ directly. Among these, revolutionary technologies are organ printing, cell laser printing, hydrogel and microfluid technology photopatterning [90]. Organ printing's purpose is to generate 3D vascularized human organ products suitable for clinical implantation. Industrial robotic bio-fabrication of complicated human tissues and organisms, tissue automatic clinical diagnosis, medicine detection and drug toxicity, and sophisticated in vitro human models are the main practical outputs of organ printing. Boland et al. developed a cell printer to accomplish the organ printing approach. The printer can print single cells, cellular aggregates, and the printing material, which is reversible thermal gel. The authors established the efficacy of this technology by printing a collagen tubular gel with bovine endothelial aortal cells. The researchers used a laser-backed printer to deposit micron-scale patterns of pluripotent embryonic cancer cells onto thin hydrogel layers, and cell survival was 95%. Valerie and Sangeeta changed the photolithographic processes used by silicon chip producers. It begins with the application of a thin layer of cell-loaded polymer solution to a Teflon substrate. UV light is emitted by a specific template on the thin film's surface, curing the exposed polymer within the cells. Complex 3D designs integrating different sections of the cells can be made by layering many templates on top of each other. The route map for bioprinting human hearts is depicted in Fig. 26 [91–93].

MRIs of patients are used to build a thorough three-dimensional map of the human heart that is unique to the patient. The patient's skin is sampled, and the dermal fibroblasts are removed and turned into induced pluripotent stem (iPS) cells, which can be transformed into any cell type in the human body. After that, the iPS cells are converted into contracting cardiomyocytes. Ideally, iPS cells would be reprogrammed to produce conducting pacemaker and Purkinje cells, as well as vascular system cells such as smooth muscle cells, endothelial cells, and cardiac fibroblasts. The reprogrammed cells are then blended with specially prepared bio-inks for bioprinting patient-specific human hearts, which vary based on cell type. Bio-inks are made by combining biomaterials, chemicals, growth factors,

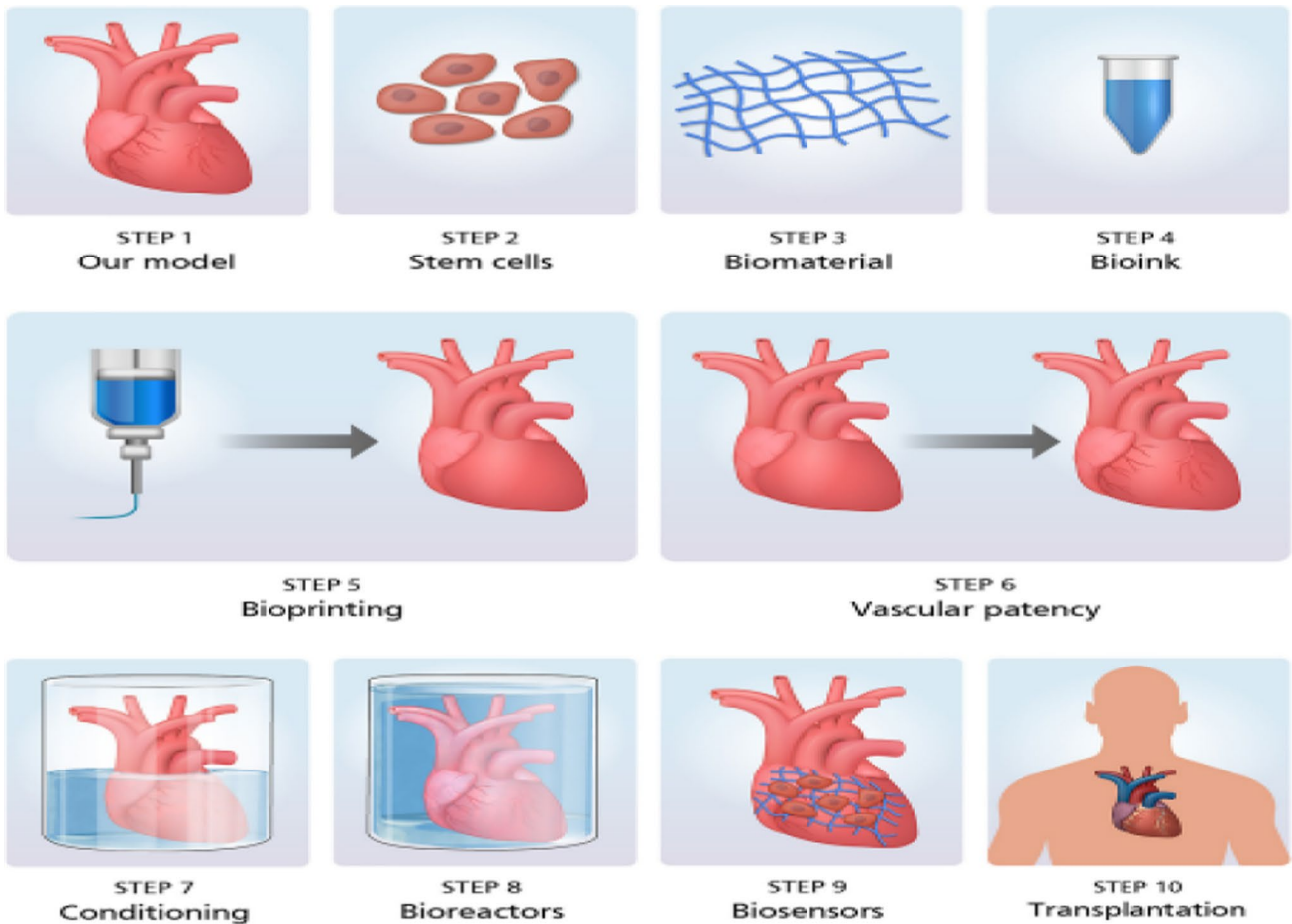


Fig. 26 A bio-printing process is employed to model the heart with patient MRI photos. Dermal fibroblast is extracted and transformed into iPS cells and cardiomyocytes from patient biopsies of the skin.

Cardiomyocytes are mixed and employed in the bioprinting of individual patient hearts. Bio-printed hearts are conditioned and transplanted by bioreactors [93]

and hormones in novel ways. Following printing, the heart is cultured in static circumstances for several days before being transferred to a bioreactor for bioreactor culture and conditioning to aid in cardiac muscle development and maturation. Following bioreactor conditioning, bio-printed hearts are ready for clinical transplantation. Specific sensors are utilized to record metrics such as left ventricular pressure and electrocardiogram properties to monitor cell and tissue survival as well as functional performance in real time. The hearts are immunologically acceptable and do not require immune suppression medication because they were bio-printed using autologous patient cells [94, 95].

Conclusions and Future Prospects

Despite significant progress in the field of bone tissue regeneration in recent years, current therapies, such as bone grafts, still have many limitations [96]. Furthermore,

despite significant advances in material science innovation in the context of bone replacement therapies, no adequate bone alternative has been advanced, and thus, large bone defects/injuries continue to pose a significant challenge for Orthopaedic and reconstructive surgeons [97–104]. TE is emerging as a viable alternative to current bone regeneration/substitution therapies. Many researchers have found that non-conventional-fabricated scaffolds improve tissue regeneration when compared to conventionally fabricated scaffolds. RP technologies have overcome some of the shortcomings of traditional scaffold manufacturing procedures [105–110]. Different RP procedures offer unique traits and benefits, yet they also have flaws and issues. SLA’s main drawbacks are limited material options and poor biomechanical strength of leftovers [111, 112]. New photocurable polymers or component combinations must be developed to overcome these disadvantages. Even while DLP has not yet been applied in the manufacturing of bone tissue, it and other new technologies have a bright future. SLS and

3DP are caused by weak structures. Some topics and fields remain undiscovered. (1) Despite the fact that RP technologies have the theoretical capability of manufacturing carefully regulated scaffolds with uniformly distributed pores, there have been few reports or research comparing the osteogenic capabilities of RP technologies with previous approaches. Furthermore, most of the research is still in the experimental phase, demanding rigorous testing before clinical use. (2) The natural bone structure is not uniform. The scaffolding design must also be altered. (3) Because most RP processes are harsh, physiologically active components can only be introduced into scaffolds after they have been post-processed. (4) Due to a paucity of bone transplant possibilities, treating mass bone shortages remains a difficulty in bone tissue repair to break through the "development bottleneck," RP-based 3D biological printing technology and nanotechnology will be important. Finally, the selection of appropriate biomaterials, preparation methods, and scaffold design are crucial. The development of new materials and techniques, the optimization of scaffolds, the control of interfaces, and the introduction of physiologically active compounds will be the most difficult challenges for bone tissue engineering. The clinical transplant chimera, consisting of a lion's head, a goat's body, and a snake tail, demonstrates that tissue engineering is a multidisciplinary field.

Funding This research received no financial support by any funding organization.

Declarations

Conflict of interest The authors don't have any conflict of interest nor have any conflict between any institution and between, both the author.

References

1. S. Gómez, M.D. Vlad, J. López, E. Fernández, Design and properties of 3d scaffolds for bone tissue engineering. *Acta biomaterialia*. **42**, 341–350 (2016)
2. A. Boccaccio, M. Fiorentino, M. Gattullo, V.M. Manghisi, G. Monno, *A computational mechanobiological approach geometry modelling of regular scaffolds for bone tissue engineering* (Springer, Cham, 2019)
3. J. A. Leboucher, C. R. Van Donkelaar, B. Van Rietbergen, J. Donners, and R. Huiskes, "Design and characterization of a scaffold for bone tissue engineering," pp. 1–46, 2020
4. L. Polo-Corrales, M. Latorre-Esteves, J.E. Ramirez-Vick, Scaffold design for bone regeneration. *J. Nanosci. Nanotechnol.* **14**(1), 15–56 (2014). <https://doi.org/10.1166/jnn.2014.9127>
5. T. Tariverdian, F. Sefat, M. Gelinsky, M. Mozafari, Scaffold for bone tissue engineering, in *Handbook of tissue engineering Scaffolds*. (Elsevier, 2019), pp.189–209. <https://doi.org/10.1016/B978-0-08-102563-5.00010-1>
6. M. Ansari, Bone tissue regeneration: biology, strategies and interface studies. *Prog. Biomater.* **8**(4), 223–237 (2019). <https://doi.org/10.1007/s40204-019-00125-z>
7. R. Florencio-Silva, G. Rodrigues, Biology of bone tissue: structure, function, and factors that influence bone cells. *BioMed Res. Int.* **2015**, 1–17 (2015). <https://doi.org/10.1155/2015/421746>
8. J.M. Kim, C. Lin, Z. Stavre, M.B. Greenblatt, J.H. Shim, Osteoblast-osteoclast communication and bone homeostasis. *Cells* **9**(9), 1–14 (2020). <https://doi.org/10.3390/cells9092073>
9. C. Vrahnas, N.A. Sims, Basic Aspects of Osteoblast Function, in *Osteoporosis: pathophysiology and clinical management*. ed. by B.Z. Leder, M.N. Wein (Springer, Cham, 2020), pp.1–16. https://doi.org/10.1007/978-3-319-69287-6_1
10. H.K. Väänänen, H. Zhao, M. Mulari, J.M. Halleen, The cell biology of osteoclast function. *J. Cell Sci.* **113**(3), 377–381 (2000). <https://doi.org/10.1242/jcs.113.3.377>
11. K. Henriksen, J. Bollerslev, V. Everts, M.A. Karsdal, Osteoclast activity and subtypes as a function of physiology and pathology: implications for future treatments of osteoporosis. *Endocr. Rev.* **32**(1), 31–63 (2011). <https://doi.org/10.1210/er.2010-0006>
12. J. S. Broderick and L. Bone, "Biology of Bone Repair Types of Bone canal Lamellar Bone Woven Bone," no. March 2004, pp. 1–14, 2005
13. B. Repair, "Cellular Repair," pp. 77–86, 1997
14. H. Schell, G.N. Duda, A. Peters, S. Tsitsilonis, K.A. Johnson, K. Schmidt-Bleek, The haematoma and its role in bone healing. *J. Exp. Orthopaed.* (2017). <https://doi.org/10.1186/s40634-017-0079-3>
15. T.A. Einhorn, L.C. Gerstenfeld, Fracture healing: mechanisms and interventions. *Nat. Rev. Rheumatol.* **11**(1), 45–54 (2015). <https://doi.org/10.1038/nrrheum.2014.164>
16. J.H. Zeng et al., Scaffolds for the repair of bone defects in clinical studies: A systematic review. *J. Orthop. Surg. Res.* **13**(1), 1–14 (2018). <https://doi.org/10.1186/s13018-018-0724-2>
17. P. Lichte, H.C. Pape, T. Pufe, P. Kobbe, H. Fischer, Scaffolds for bone healing: concepts, materials and evidence. *Injury* **42**(6), 569–573 (2011). <https://doi.org/10.1016/j.injury.2011.03.033>
18. E. Sachlos, J.T. Czernuszka, S. Gogolewski, M. Dalby, Making tissue engineering scaffolds work. review on the application of solid freeform fabrication technology to the production of tissue engineering scaffolds. *Eur. Cells Mater.* **5**, 29–40 (2003). <https://doi.org/10.22203/ecm.v005a03>
19. Z. Yang, H. Peng, W. Wang, T. Liu, Crystallization behavior of poly(ϵ -caprolactone)/layered double hydroxide nanocomposites. *J. Appl. Polym. Sci.* **116**(5), 2658–2667 (2010). <https://doi.org/10.1002/app>
20. F. Shapiro, Bone development and its relation to fracture repair. The role of mesenchymal osteoblasts and surface osteoblasts. *Eur. Cells Mater.* **15**, 53–76 (2008). <https://doi.org/10.22203/ecm.v015a05>
21. Q. Lv, Q.L. Feng, Preparation of 3-D regenerated fibroin scaffolds with freeze drying method and freeze drying/foaming technique. *J. Mater. Sci. Mater. Med.* **17**(12), 1349–1356 (2006). <https://doi.org/10.1007/s10856-006-0610-z>
22. P. Carter, N. Bhattarai, Bioscaffolds: fabrication and performance, in *Engineered Biomimicry*. (Elsevier, 2013), pp.161–188. <https://doi.org/10.1016/B978-0-12-415995-2.00007-6>
23. F. Dehghani, N. Annabi, Engineering porous scaffolds using gas-based techniques. *Curr. Opin. Biotechnol.* **22**(5), 661–666 (2011). <https://doi.org/10.1016/j.copbio.2011.04.005>
24. A.D. Bagde et al., State of the art technology for bone tissue engineering and drug delivery. *Irbm* **40**(3), 133–144 (2019). <https://doi.org/10.1016/j.irbm.2019.03.001>
25. A. Eltom, G. Zhong, A. Muhammad, Scaffold techniques and designs in tissue engineering functions and purposes: a review.

- Adv. Mater. Sci. Eng. **2019**, 1–13 (2019). <https://doi.org/10.1155/2019/3429527>
26. S. Taherkhani, F. Moztarzadeh, Fabrication of a poly(ϵ -caprolactone)/starch nanocomposite scaffold with a solvent-casting/salt-leaching technique for bone tissue engineering applications. *J. Appl. Polym. Sci.* **133**(23), 19–21 (2016). <https://doi.org/10.1002/app.43523>
 27. E. Yilmaz and M. Soylak, Functionalized nanomaterials for sample preparation methods. Elsevier Inc., 2019.
 28. S.W. Suh et al., Effect of different particles on cell proliferation in polymer scaffolds using a solvent-casting and particulate leaching technique. *ASAIJ*. **48**(5), 460–464 (2002). <https://doi.org/10.1097/00002480-200209000-00003>
 29. N.F.M. Nasir, S.F. Khan, E.M. Cheng, J.S. Baling, N.A.M. Amin, M.S.A. Majid, Preliminary study of trong clay – ha bone scaffold fabrication using solvent casting/particulate leaching method and indirect 3d-printing technique. *J. Eng. Res. Educ.* **10**, 83–90 (2018)
 30. M. Mehrabian, M. Nasr-Esfahani, HA/nylon 6,6 porous scaffolds fabricated by salt-leaching/solvent casting technique: effect of nano-sized filler content on scaffold properties. *Int. J. Nanomedicine* **6**, 1651–1659 (2011)
 31. J. Kundu, F. Pati, Y. Hun Jeong, and D. W. Cho, Biomaterials for Biofabrication of 3D Tissue Scaffolds, First Edit. Elsevier Inc., 2013.
 32. J. Alvarado, R. Maldonado, J. Marxuach, and R. Otero, “Biomechanics of the hip and knee prosthesis,” *Appl. Eng. Mech.*, no. December, pp. 6–22, 2003.
 33. V. Melčová et al., Fdm 3d printed composites for bone tissue engineering based on plasticized poly(3-hydroxybutyrate)/poly(d, l-lactide) blends. *Polymers (Basel)* **12**(12), 1–19 (2020). <https://doi.org/10.3390/polym12122806>
 34. S.A. Poursamar, J. Hatami, A.N. Lehner, C.L. Da Silva, F.C. Ferreira, A.P.M. Antunes, Gelatin porous scaffolds fabricated using a modified gas foaming technique: characterisation and cytotoxicity assessment. *Mater. Sci. Eng. C* **48**, 63–70 (2015). <https://doi.org/10.1016/j.msec.2014.10.074>
 35. T. Lu, Y. Li, T. Chen, Techniques for fabrication and construction of three-dimensional scaffolds for tissue engineering. *Int. J. Nanomed.* **8**, 337–350 (2013). <https://doi.org/10.2147/IJN.S38635>
 36. T. L. Landsman, A. C. Weems, S. M. Hasan, R. S. Thompson, T. S. Wilson, and D. J. Maitland, *Embollic Applications of Shape Memory Polyurethane Scaffolds*. Elsevier Ltd, 2016
 37. Hale Karakaş, “electrospinning of nanofibers and their applications - PDF Drive,” MDT “Electrospinning,” vol. 3, pp. 1–35, 2012, [Online]. Available: <http://www.pdfdrive.net/electrospinning-of-nanofibers-and-their-applications-e34353447.html>.
 38. A. Chanthakulchan, P. Koomsap, K. Auysan, P. Supaphol, Development of an electrospinning-based rapid prototyping for scaffold fabrication. *Rapid Prototyp. J.* **21**(3), 329–339 (2015). <https://doi.org/10.1108/RPJ-11-2013-0119>
 39. B. Arifvianto, J. Zhou, Fabrication of metallic biomedical scaffolds with the space holder method: a review. *Materials (Basel)* **7**(5), 3588–3622 (2014). <https://doi.org/10.3390/ma7053588>
 40. L. F. Francis, *Powder Processes*. 2016
 41. A. Chláková, J. Wiener, J.M. Luthuli, V. Zajícová, Dyeing of glass fibres by the sol gel method. *Autex Res. J.* **11**(1), 18–23 (2011)
 42. Barby D., Haq Z., inventors. Tough reinforced open porous polymer foams via concentrated emulsion templating, 1982. European patent 60138
 43. K. Dixit, A. Raichur, N. Sinha, Polymer coated and nanofiber reinforced functionally graded bioactive glass scaffolds fabricated using additive manufacturing. *IEEE Trans. Nanobiosci.* **434**, 1–33 (2021)
 44. G. Turnbull et al., 3D bioactive composite scaffolds for bone tissue engineering. *Bioact. Mater.* **3**(3), 278–314 (2018). <https://doi.org/10.1016/j.bioactmat.2017.10.001>
 45. M. Saman Naghieh, M.K.R. Sarker, A. McInnes, X. Chen, Modeling of the mechanical behavior of 3D bioplotting scaffolds considering the penetration in interlocked strands. *Appl. Sci.* **8**(9), 1422 (2018). <https://doi.org/10.3390/app8091422>
 46. A.V. Do, B. Khorsand, S.M. Geary, A.K. Salem, 3D Printing of scaffolds for tissue regeneration applications. *Adv. Healthc. Mater.* **4**(12), 1742–1762 (2015). <https://doi.org/10.1002/adhm.201500168>
 47. J. An, J.E.M. Teoh, R. Suntronnond, C.K. Chua, Design and 3D printing of scaffolds and tissues. *Engineering* **1**(2), 261–268 (2015). <https://doi.org/10.15302/J-ENG-2015061>
 48. S. Lohfeld, M.A. Tyndyk, S. Cahill, N. Flaherty, V. Barron, P.E. McHugh, A method to fabricate small features on scaffolds for tissue engineering via selective laser sintering. *J. Biomed. Sci. Eng.* **03**(02), 138–147 (2010). <https://doi.org/10.4236/jbise.2010.32019>
 49. P. Rider, Ž Kačarević, S. Alkildani, S. Retnasingh, R. Schnettler, M. Barbeck, Additive manufacturing for guided bone regeneration: a perspective for alveolar ridge augmentation. *Int. J. Mol. Sci.* **19**(11), 3308 (2018). <https://doi.org/10.3390/ijms19113308>
 50. K.W. Lee, S. Wang, B.C. Fox, E.L. Ritman, M.J. Yaszemski, L. Lu, Poly(propylene fumarate) bone tissue engineering scaffold fabrication using stereolithography: Effects of resin formulations and laser parameters. *Biomacromol* **8**(4), 1077–1084 (2007). <https://doi.org/10.1021/bm060834v>
 51. E.N. Antonov et al., Three-dimensional bioactive and biodegradable scaffolds fabricated by surface-selective laser sintering. *Adv. Mater.* **17**(3), 327–330 (2005). <https://doi.org/10.1002/adma.200400838>
 52. F.N. Alaribe, S.L. Manoto, S.C.K.M. Motaung, Scaffolds from biomaterials: advantages and limitations in bone and tissue engineering. *Biologia (Bratisl)* **71**(4), 353–366 (2016). <https://doi.org/10.1515/biolog-2016-0056>
 53. C.S. Ranucci, A. Kumar, S.P. Batra, P.V. Moghe, Control of hepatocyte function on collagen foams: Sizing matrix pores toward selective induction of 2-D and 3-D cellular morphogenesis. *Biomaterials* **21**(8), 783–793 (2000). [https://doi.org/10.1016/S0142-9612\(99\)00238-0](https://doi.org/10.1016/S0142-9612(99)00238-0)
 54. K.H. Bouhadir, D.D.J. Mooney, Promoting angiogenesis in engineered tissues. *J. Drug Target.* **9**(6), 397–406 (2001). <https://doi.org/10.3109/10611860108998775>
 55. R.K. Birla, S.K. Williams, 3D bioprinting and its potential impact on cardiac failure treatment: an industry perspective. *APL Bioeng.* **4**(1), 010903 (2020). <https://doi.org/10.1063/1.5128371>
 56. W. Li, C.T. Laurencin, E.J. Caterson, R.S. Tuan, F.K. Ko, Electrospun nanofibrous structure: a novel scaffold for tissue engineering. *J. Biomed. Mater. Res.* **60**, 613–621 (2002)
 57. K. Dixit, P. Gupta, S. Kamle, N. Sinha, Structural analysis of porous bioactive glass scaffolds using micro-computed tomographic images. *J. Mater. Sci.* **55**(27), 12705–12724 (2020)
 58. J.A. Matthews, G.E. Wnek, D.G. Simpson, G.L. Bowlin, Electrospinning of collagen nanofibers. *Biomacromol* **3**, 232–238 (2002)
 59. S.H. Kim, Y.S. Nam, T.S. Lee, W.H. Park, Silk fibroin nanofiber. Electrospinning, properties, and structure. *Polym. J.* **35**(2), 185–190 (2003). <https://doi.org/10.1295/polymj.35.185>
 60. W.J. Li, R.S. Tuan, Fabrication and application of nanofibrous scaffolds in tissue engineering. *Curr. Protocols Cell Biol.* (2009). <https://doi.org/10.1002/0471143030.cb2502s42>
 61. D. Liang, B.S. Hsiao, B. Chu, Functional electrospun nanofibrous scaffolds for biomedical applications. *Adv. Drug Delivery Rev.* **59**(14), 1392–1412 (2007). <https://doi.org/10.1016/j.addr.2007.04.021>

62. M.F. Leong, M.Z. Rasheed, T.C. Lim, K.S. Chian, *In vitro* cell infiltration and *in vivo* cell in filtration and vascularization in fibrous highly porous poly (D, L-Lactic acid) scaffold fabrication by electrospinning technique. *J Biomed Res A*. **91**, 231–240 (2008)
63. B.M. Baker, A.O. Gee, R.B. Metter, A.S. Nathan, R.A. Marklein, J.A. Burdick, R.L. Mauck, The potential to improve cell infiltration in composite fiber-aligned electrospun scaffolds by the selective removal of sacrificial fibers. *Biomaterials* **29**, 2348–2358 (2008)
64. Z.R. Domingues, M.E. Cortés, T.A. Gomes, H.F. Diniz, C.S. Freitas, J.B. Gomes, A.M. Faria, R.D. Sinisterra, Bioactive glass as a drug delivery system of tetracycline and tetracycline associated with cyclodextrin. *Biomaterials* **25**, 327–333 (2004)
65. A. Ulatowski-Jarza, D. Andrzejewski, H. Podbielska, K. Maruszewski, W. Strek, Advantages of sol-gel technologies for biomedical applications. *Proc SPIE*. **3567**, 50 (1999)
66. S. Di Nunzio, C. Vitale-Brovarone, S. Spriano, D. Milanese, E. Verne, V. Bergo, G. Maina, P. Spinelli, Silver containing bioactive glasses prepared by molten salt ionexchange. *J. Eur. Ceram. Soc.* **24**, 2935–2942 (2004)
67. S. Kimakhe, S. Bohic, C. Larosse, A. Reynaud, P. Pilet, B. Giumelli, D. Heymann, G. Daculsi, Biological activities of sustained polymixin B release from calcium phosphate biomaterial prepared by dynamic compaction: an *in vitro* study. *J. Biomed. Mater. Res.* **47**, 18–27 (1999)
68. Y.S. Nam, T.G. Park, Biodegradable polymeric microcellular foams by modified thermally induced phase separation method. *Biomaterials* **20**, 1783–1790 (1999)
69. L.A. Smith, J.A. Beck, P.X. Ma, Nano fibrous scaffolds and their biological effects, in *Tissue, cell and organ engineering*. ed. by C. Kumar (Wiley-VCH, Weinheim, 2006), p.195
70. P.X. Ma, R. Zhang, Microtubular architecture of biodegradable polymer scaffolds. *J. Biomed. Mater. Res.* **56**(4), 469–477 (2001)
71. A.R. Boccaccini, I. Notinger, V. Maquet, R. Jerome, Bioresorbable and bioactive composite materials based on polylactide foams filled with and coated by Bioglass particles for tissue engineering application. *J. Mater. Sci. Mater. Med.* **14**, 443–450 (2003)
72. Y.S. Nam, T.G. Park, Porous biodegradable polymeric scaffolds prepared by thermally induced phase separation. *J. Biomed. Mater. Res.* **47**, 8–17 (1999)
73. R.C. Thompson, M.C. Wake, M.J. Yasemski, A.G. Mikos, *Adv. Polym. Sci.* **122**, 245–274 (1995)
74. B. Kim, D.J. Mooney, Engineering smooth muscle tissue with a predefined structure. *J. Biomed. Mater. Res.* **41**, 322–332 (1998)
75. L.G. Cima, J.P. Vacanti, C. Vacanti, D. Ingber, D. Mooney, R. Langer, Tissue engineering by cell transplantation using degradable polymer substrates. *J. Biomech. Eng.* **113**(2), 143–151 (1991)
76. A.G. Mikos, Y. Bao, L.G. Cima, D.E. Ingber, J.P. Vacanti, R. Langer, Preparation of poly (glycolic acid) bonded fiber structures for cell attachment and transplantation. *J. Biomed. Mater. Res.* **27**(2), 183–189 (1993)
77. D. Eberli, F.L. Freitas, A. Atala, J.J. Yoo, Composite scaffolds for the engineering of hollow organs and tissues. *Methods* **47**(2), 109–115 (2009)
78. L. Moroni, D. Hamann, L. Paoluzzi, J. Pieper, J.R. de Wijn, C.A. Van Blitterswijk, Regenerating articular tissue by converging technologies. *PLoS ONE* **3**(8), e3032 (2008)
79. A.M. Martins, Q.P. Pham, P.B. Malafaya, R.A. Sousa, M.E. Gomes, R.M. Raphael, F.K. Kapsner, R.L. Reis, A.G. Mikos, The role of lipase and alpha-amylase in the degradation of starch/poly(varepsilon-caprolactone) fiber meshes and the osteogenic differentiation of cultured marrow stromal cells. *Tissue Eng. Part A*. **15**(2), 295–305 (2009)
80. Y. Ikada, Scope of tissue engineering, in *Tissue Engineering, fundamental and applications*. ed. by Y. Ikada (Academic Press, Waltham, 2006), p.29
81. G. Chen, T. Ushida, T. Tateishi, Development of biodegradable porous scaffolds for tissue engineering. *Mater. Sci. Eng. C*. **17**, 63–69 (2002)
82. T.M.G. Chu, D.G. Orton, S.J. Hollister, S.E. Feinberg, J.W. Halloran, Mechanical and *in vivo* performance of Hydroxyapatite implants with controlled architectures. *Biomaterials* **23**, 1283–1293 (2002)
83. Hollister S. J., Chu T. M., Halloran J. W., Feinberg SE. Design and manufacture of bone replacement scaffolds. In: Cowen S (ed.), *Bone Mechanics*. Boca Raton, FL: CRC Press, 2000, in press
84. S.J. Hollister, R.D. Maddox, J.M. Taboas, Optimal design and fabrication of scaffolds to mimic tissue properties and satisfy biological constraints. *Biomaterials* **23**(20), 4095–4103 (2002)
85. D.W. Huttmacher, Scaffolds in tissue engineering bone and cartilage. *Biomaterials* **21**, 2529–2543 (2000)
86. S. Yang, K.F. Leong, D. Zhaohui, C.K. Chua, The design of scaffolds for use in tissue engineering. Part II. Rapid prototyping techniques. *Tissue Eng.* **8**(1), 1–11 (2002). <https://doi.org/10.1089/107632702753503009>
87. E. Sachlos, J.T. Czernuszka, Making tissue engineering scaffolds work. Review: the application of solid freeform fabrication technology to the production of tissue engineering scaffolds. *Eur. Cells Mater.* **5**, 29–40 (2003). <https://doi.org/10.22203/eCM.v005a03>
88. C.M. Cheah, C.K. Chua, K.F. Leong, S.W. Chua, Development of a tissue engineering scaffold structure library for rapid prototyping. Part 1: investigation and classification. *Int. J. Adv. Manuf. Technol.* **21**(4), 291–301 (2003)
89. D.W. Huttmacher, M. Sittinger, M.V. Risbud, Scaffold-based tissue engineering: rationale for computeraided design and solid free-form fabrication systems. *Trends Biotechnol.* **22**(7), 354–362 (2004)
90. M. Vladimirov, B. Thomas, T. Thomas, F. Gabor, R.M. Roger, Organ printing: computer-aided jet-based 3D tissue engineering. *Trends Biotechnol.* **21**(4), 157–161 (2003)
91. V. Maquet, R. Jerome, Design of macroporous biodegradable polymer scaffolds for cell transplantations. *Mater Sci Forum*. **250**, 15–24 (1997)
92. D.W. Huttmacher, Scaffold in tissue engineering bone and cartilage. *Biomaterials* **21**, 2529–2543 (2000)
93. D.W. Huttmacher, Scaffold design and fabrication technologies for engineering tissues: state of the art and future perspectives. *J. Biomat. Sci. Polym.* **12**, 107–124 (2001)
94. S. Partap, J.A. Darr, I.U. Rehman, J.R. Jones, Supercritical carbon dioxide in water emulsion-templated synthesis of porous calcium alginate hydrogels. *Adv. Mater.* **18**, 501–504 (2006)
95. K. Dixit, N. Sinha, Compressive strength enhancement of carbon nanotube reinforced 13–93B1 bioactive glass scaffolds. *J. Nanosci. Nanotechnol.* **19**, 2738–2746 (2019)
96. B. Thavorniyutikarn, N. Chantarapanich, K. Sitthiseripratip, G.A. Thouas, Q. Chen, Bone tissue engineering scaffolding: computer-aided scaffolding techniques. *Prog. Biomater.* **3**(2–4), 61–102 (2014). <https://doi.org/10.1007/s40204-014-0026-7>
97. B. Subia, J. Kundu, Biomaterial Scaffold Fabrication Techniques for Potential Tissue Engineering Applications, in *Tissue Engineering*. ed. by D. Eberli (InTech, 2010). <https://doi.org/10.5772/8581>
98. H.A. Declercq, T. Desmet, P. Dubrue, M.J. Cornelissen, The role of scaffold architecture and composition on the bone formation by adipose-derived stem cells. *Tissue Eng. - Part A* **20**(1–2), 434–444 (2014). <https://doi.org/10.1089/ten.tea.2013.0179>

99. N. Poomathi et al., 3D printing in tissue engineering: a state of the art review of technologies and biomaterials. *Rapid Prototyp. J.* **26**(7), 1313–1334 (2020). <https://doi.org/10.1108/RPJ-08-2018-0217>
100. R. Singh, S. Singh, and M. S. J. Hashmi, *Implant Materials and Their Processing Technologies*. Elsevier Ltd., 2016.
101. W. Liu et al., Low-temperature deposition manufacturing: a novel and promising rapid prototyping technology for the fabrication of tissue-engineered scaffold. *Mater. Sci. Eng. C* **70**, 976–982 (2017). <https://doi.org/10.1016/j.msec.2016.04.014>
102. Y. Liu, S. Fang, Z. Han, D. Liu, Y. Liu, Q. Hu, The research on a new feeding device of low-temperature deposition for fabricating tissue engineering scaffolds. *Key Eng. Mater.* **522**, 92–96 (2012). <https://doi.org/10.4028/www.scientific.net/KEM.522.92>
103. C. Liu, J. Tong, J. Ma, D. Wang, X. Feng, Y. Liu, Z. Chen, C. Lao, Low-temperature deposition manufacturing: a versatile material extrusion-based 3D printing technology for fabricating hierarchically porous materials. *J. Nanomater.* **2019**, 1–14 (2019). <https://doi.org/10.1155/2019/1291067>
104. W.Y. Yeong, C.K. Chua, K.F. Leong, M. Chandrasekaran, Rapid prototyping in tissue engineering: challenges and potential. *Trends Biotechnol.* **22**(12), 643–652 (2004). <https://doi.org/10.1016/j.tibtech.2004.10.004>
105. T. Phattanaphibul, P. Koomsap, I. Idram, S. Nachaisit, Development of SVM rapid prototyping for scaffold fabrication. *Rapid Prototyp. J.* **20**(2), 90–104 (2014). <https://doi.org/10.1108/RPJ-05-2012-0042>
106. P. Koomsap and T. Phattanaphibul, “Exploring SVM Rapid Prototyping in Scaffold Fabrication,” vol. 4, pp. 71–76, 2011
107. T.B.F. Woodfield, J. Malda, J. De Wijn, F. Pétters, J. Riesle, C.A. Van Blitterswijk, Design of porous scaffolds for cartilage tissue engineering using a three-dimensional fiber-deposition technique. *Biomaterials* **25**(18), 4149–4161 (2004). <https://doi.org/10.1016/j.biomaterials.2003.10.056>
108. F. Wang et al., Precision extruding deposition and characterization of cellular poly-ε-caprolactone tissue scaffolds. *Rapid Prototyp. J.* **10**(1), 42–49 (2004). <https://doi.org/10.1108/13552540410512525>
109. G. Vozzi, C. Flaim, A. Ahluwalia, S. Bhatia, Fabrication of PLGA scaffolds using soft lithography and microsyringe deposition. *Biomaterials* **24**(14), 2533–2540 (2003). [https://doi.org/10.1016/S0142-9612\(03\)00052-8](https://doi.org/10.1016/S0142-9612(03)00052-8)
110. G. Vozzi, A. Previti, D. De Rossi, A. Ahluwalia, Microsyringe-based deposition of two-dimensional and three-dimensional polymer scaffolds with a well-defined geometry for application to tissue engineering. *Tissue Eng.* **8**(6), 1089–1098 (2002). <https://doi.org/10.1089/107632702320934182>
111. A. Neto, J. Ferreira, Synthetic and marine-derived porous scaffolds for bone tissue engineering. *Materials* **11**(9), 1702 (2018). <https://doi.org/10.3390/ma11091702>
112. K. Dixit, N. Sinha, “Additive manufacturing of carbon nanotube reinforced bioactive glass scaffolds for bone tissue engineering,” *ASME. J. Eng. Sci. Med. Diagnostics Ther.* **4**(4), 1–8 (2021)

Publisher’s Note Springer Nature remains neutral with regard to jurisdictional claims in published maps and institutional affiliations.

Springer Nature or its licensor holds exclusive rights to this article under a publishing agreement with the author(s) or other rightsholder(s); author self-archiving of the accepted manuscript version of this article is solely governed by the terms of such publishing agreement and applicable law.